Utility Based Cooperative Resource Sharing in Symbiotic Radio aided Internet of Things Networks

Wei Liang[1,2,3] *Member, IEEE*, Shuhui Wen[1] *Member, IEEE*, Soon Xin Ng[4] *Member, IEEE*, Jiankang Zhang[5] *Member, IEEE*
[1]School of Electronic and Information, Northwestern Polytechnical University, China.
[2]The State Key Laboratory of Integrated Services Networks, Xidian University, China.
[3]The Research & Development Institute of Northwestern Polytechnical University in Shenzhen, China.
[4]School of Electronics and Computer Science, University of Southampton, U.K.
[5] Department of Computing and Informatics, Bournemouth University, U.K.

***Abstract*—Symbiotic radio (SR) is a key technique to solve the energy shortage and spectrum limitation of the future Internet of Things (IoT). In the SR-aided IoT networks supporting energy harvesting (EH), we study the cooperation schemes and offloading strategy between the primary users (PUs), IoT devices and the base station (BS) for reasonably allocating the spectrum, power and time resources. Considering the monetary transactions between the PUs and IoT devices, two cooperation schemes, namely the "Preferential Scenario" and the "No-Preferential Scenario", are proposed. In the "Preferential Scenario", based on the final strategy, the IoT devices use the purchased spectrum and power to offload their own tasks to the BS after assisting the cooperative PUs to offload during a certain time slot. Due to the assistance of IoT devices for the PUs, IoT devices enjoy a discount when paying for the purchased spectrum and power. In the "No-Preferential Scenario", the IoT devices and the cooperative PUs offload tasks to the BS together in a certain time slot according to the offloading strategy. The spectrum and power used by the IoT devices are purchased at the original price without a discount. For each scenario, we study the utility maximization problem of the PUs, where the utility of PUs includes the transmission rates and income. The utility based resource sharing algorithm is proposed to obtain an approximately optimal resource allocation scheme. Our simulation results indicate that the proposed algorithm provides good performances for both scenarios, while each scenario applying the proposed algorithm has its own advantages.**

***Index Terms*—Internet of Things, symbiotic radio, backscatter communication, energy harvesting, mobile edge computing, offloading strategy.**

I. Introduction

The global COVID-19 pandemic accelerates the growth of Internet of Things (IoT) applications, including the smart medical care, smart retail, smart transportation and other IoT applications [1]–[5]. Faced with the continuous growth of IoT devices, the insufficient spectrum and energy resources become even more scarce, resulting in the problem of energy shortage and spectrum limitation for the IoT [6]–[9].

Recently, the backscatter communication (BC) technique, which could solve the problem of energy shortage for the IoT, attracts a large number of researchers [10]–[15]. A typical example is the ambient backscatter communication (AmBC). Applying this technique, the passive backscatter devices (BDs) could transmit their own tasks to the corresponding receivers by modulating and reflecting the environmental radio frequency (RF) signals, including the TV signals, WIFI signals, cellular signals, etc [10]–[12]. Compared with the conventional communication using the active transmitters, the BC technique improves the energy utilization of IoT. However, due to the influence of unstable environment RF signals, the BC technique only supports the short distance communication, and it is difficult to achieve the highly reliable communication. Liu *et al.* [13] developed a novel hybrid scheme that integrated the BC and the harvest-then-transmit (HTT) protocol, and investigated the sum-throughput maximization problem of the secondary system. Li *et al.* [14] investigated the physical layer security of the AmBC systems, and proposed an artificial noise scheme. Toro *et al.* [15] studied the BC that enabled green IoT through joint wireless communication and sensing, and proposed that the IoT devices might operate without batteries.

Similarly, energy harvesting (EH) has been studied as another key technique to solve the problem of energy shortage [16]–[18]. Applying this technique, IoT devices could harvest energy/power from the ambient RF signals, and then transmit tasks to the receiver using the harvested energy/power. Chu *et al.* [19] investigated a wireless powered intelligent radio environment, where the fractional non-linear EH was proposed to enable an intelligent reflecting surface (IRS) assisted wireless powered IoT network. The purpose was to improve the overall performance of the considered network by maximizing the sum throughput. Zhang *et al.* [20] proposed an EH multi-codebook based BC scheme to minimize the energy consumption of backscattering data. Xiao *et al.* [21] considered an unmanned aerial vehicle (UAV)-assisted EH network, and solved the problems of spectrum scarcity and energy shortage for UAV communication. In the conceived network, the UAV performed spectrum sensing and communicating with the receiver and could replenish energy actively for transmission by harvesting renewable energy.

However, the above techniques still could not solve the spectrum limitation of IoT. Faced with the spectrum limitation, cognitive radio (CR) is widely studied, where the spectrum sensing technique is applied to find the idle spectrum [22]–[25]. In the CR networks, the secondary users could use

The work was supported by the Foundation of State Key Laboratory of Integrated Services Networks of Xidian University under Grant ISN22-03, and in pat by the Shenzhen Science and Technology program under Grant JCYJ20210324121006017 and in part by National Nature Science Foundation of China under Gants 62101450.

the authorized spectrum of primary users (PUs). Meanwhile, the interference between users is inevitable, which limits the improvement of spectrum utilization. Pei *et al.* [26] investigated the sensing-access strategies and the sensing order that could achieve the maximum energy efficiency in CR networks. Wang *et al.* [27] proposed a novel joint power and channel allocation scheme that improved the overall network throughput and reduced the average power consumption through a distributed pricing approach. Xu *et al.* [28] investigated the resource allocation for IRS assisted full-duplex CR systems for maximization the total spectral efficiency of the secondary system. However, faced with a large number of IoT access, the conventional CR networks have been unable to satisfy the spectrum requirements for users.

A new technique, symbiotic radio (SR), has recently attracted some attentions. Combining the advantages of BC and CR techniques, SR is also known as the cognitive backscatter communication, and could solve the problem of energy shortage and spectrum limitation of the IoT [29]–[33]. Compared with the BC technique, the BDs in the SR networks could modulate and reflect the RF signals of the primary transmitters to support the long distance and highly reliable communication. By comparing with the CR's framework, SR has the primary and secondary systems. In particular, the SR technique supports the communication between the primary and secondary transmitters, while the interference between users could be avoided [32], [34]–[37]. Long *et al.* [34] proposed a SR system supporting passive IoT, and investigated two practical setups, namely parasitic SR and commensal SR. The problem of sum-rate maximization and transmission power minimization were studied, and the semidefinite relaxation technique was applied to solve these problems. Liu *et al.* [35] proposed a SR system for multi-user random access, where a method to avoid interference between multiple reflected signals was proposed. Zhang *et al.* [36] studied the user association problem in symbiotic radio networks, where an IoT network parasitized in a primary cellular network. In the conceived networks, the objective of user association was to link each IoT device to an appropriate cellular user by maximizing the sum rates of all IoT devices. Zhang *et al.* [37] proposed a novel reconfigurable intelligent surface (RIS)-assisted SR system, and purposed to minimize the total transmission power at the primary transmitter. The RIS was the secondary transmitter, which could send messages to the corresponding receiver, and could enhance the primary transmission by intelligently reconfiguring the wireless environment. In these research works, the main concern was the downlink transmission of users.

With the emergence of mobile edge computing (MEC), the mobile users with the limited resource could offload computation tasks to the MEC server, which has attracted many researchers to learn the uplink transmission in the MEC scenarios [38]–[40]. However, in the IoT networks with a large number of users, the limited communication resource and MEC server's computing resource considerably affect the uplink transmission rate of users. Therefore, it is a critical solution to reasonably allocate communication and computing resources for this problem. Qian *et al.* [38] investigated the cellular assisted MEC via non-orthogonal multiple access (NOMA), where a group of edge-computing users exploited NOMA to simultaneously offload their computation-workloads to an edge-server, and conventional cellular-user allowed the edge users to reuse its authorized frequency channel for the NOMA-transmission. Wang *et al.* [39] investigated a joint task, spectrum, and transmission power allocation problem for a wireless network in which the BSs were equipped with MEC servers to jointly provide computational and communication services to users. Yang *et al.* [40] proposed a two-stage deep reinforcement learning-based offloading and resource allocation strategy to jointly optimize execution latency, processing accuracy, and energy consumption in the cooperative vehicle infrastructure system. The above works have concentrated on the system with less users, and are not suitable for the system with intensive users. In this paper, the uplink transmission with intensive users has been developed for the sake of achieving reasonably resources allocation in the MEC aided IoT networks, where users could offload their tasks to the BS integrated with a MEC server in advance.

To further improve the energy utilization of IoT, this paper studies a SR system that supports the ability of EH. In this system, the backscatter unit and EH unit are installed in each IoT device to facilitate the functions of BC and EH. The primary systems consist of the PUs and a base station (BS) integrated with a MEC server. The PUs enjoy the authorized spectrum and enough transmission power, and could communicate freely with the BS. The secondary systems consist of the IoT devices and a BS integrated with a MEC server. There is no authorized spectrum and available transmission power for the IoT devices. In order to communicate with the BS, the IoT devices could trade money with the PUs to obtain the communication resources, including the spectrum and transmission power. In the face of the requirements of IoT devices, the PUs provide two cooperation schemes, namely the "Preferential Scenario" and the "No-Preferential Scenario". In the "Preferential Scenario", for the sake of obtaining the discounts, the IoT devices firstly help the cooperative PUs to transmit the offloaded tasks to the BS, and then transmit their own offloaded tasks to the BS. In the "No-Preferential Scenario", the IoT devices purchase the spectrum and transmission power from the cooperative PUs at the original price, and offload tasks to the BS with the PUs at the same time.

The main contributions of this paper are summarized as follows:

- The novel IoT networks are investigated, where the SR technique is applied. In the conceived SR-aided IoT networks, each user would like to offload tasks to the BS that is integrated with the MEC server. The PUs has the ability to transmit tasks to the IoT devices and BS. Meanwhile, the IoT devices lack the authorized spectrum and transmission power to transmit tasks, which could be shared by the PUs. Considering the cooperation strategy between the PUs and IoT devices as well as the offloading strategy of each PU-IoT pair, two scenarios are proposed and discussed respectively, namely the "Preferential Sce-

nario" and the "No-Preferential Scenario".

- In the "Preferential Scenario", a cooperative protocol for the PUs, IoT devices and BS is proposed. The IoT devices have three work stages. Firstly, the IoT devices work as the backscatter devices to provide the backscatter link for the matched PUs, for improving the transmission rates of PUs. Meanwhile, the IoT devices harvest power from the matched PUs. Then, the harvested power is used by the IoT devices for transmitting tasks. Based on the above relationships, the monetary transactions are built. The IoT devices pay for the harvested power to the matched PUs, while the PUs gives the discount for the improved rates. For each PU-IoT pair, the PU and IoT device offload tasks to the BS during some time slot in the order.
- In the "No-Preferential Scenario", a different protocol is proposed. The IoT devices only have one work stage, namely transmitting tasks together with the matched PUs using the backscattered power. This would interfere with the transmission of the matched PUs, and lead to the decreasing of their transmission rates. For the sake of monetary benefit, the PUs suffer some degree of interference from the matched IoT devices. The monetary transactions are built between the PUs and IoT devices, where the IoT devices pay for the used power to the matched PUs. The PU and IoT device offload tasks to the BS during some time slot together.
- The sum-utility maximization problems of the PUs are studied. The utility based resources sharing algorithm is proposed to solve the matching problem of the PUs, IoT devices and BS, as well as to maximize the sum-utility of PUs. The matching between the PUs and IoT devices is to solve the monetary transactions problem, while the matching between the PU-IoT pairs and BS is to schedule a proper offloading strategy. To present an insightful analysis of the proposed algorithm, simulations are provided for both of the two scenarios while applying the proposed algorithm. Simulation results validate that the proposed algorithm has the good performance in both scenarios, and each scenario has its own advantages when applying the proposed algorithm.

The rest of this paper is organized as follows: Section II introduces the system model of the considered network. Section III and Section IV present the communication and computing models, cooperation protocols, as well as the optimized problems for the "Preferential Scenario" and the "No-Preferential Scenario". Then in Section V, the utility based resources sharing algorithm is proposed to solve the formulated problems for both scenarios, and the stability of the proposed algorithm is analysed. Simulation results and performance analysis are investigated in Section VI. Finally, the main conclusion is summarized in Section VII.

II. System Model

The system model of SR-aided IoT networks is shown in Fig. 1, in which there is one BS integrated with a MEC server, M PUs and N IoT devices. The SR-aided IoT networks consist of a primary system and a secondary system. In the primary system, the PUs are the primary transmitters (PTs). The BS integrated with a MEC Server is the primary/secondary receiver (PR/SR) in the primary/secondary system. Meanwhile, the IoT devices are treated as the secondary transmitters (STs) in the secondary system and backscatter devices (BDs) in the system of SR, respectively. In the conceived networks, each PU has the capability of local computation, authorized spectrum and stable transmission power supply, while the capabilities of local computation for the IoT devices are limited to the authorized spectrum and free transmission power.

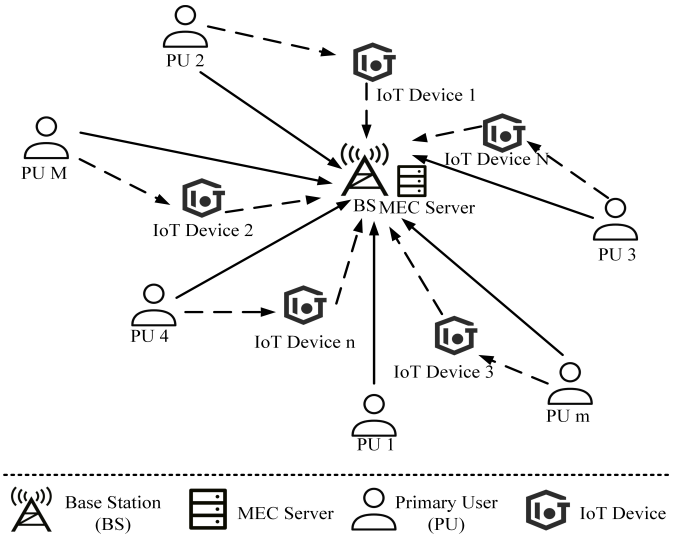

Fig. 1. System model of SR-aided IoT networks.

Each PU can offload tasks to the BS by the direct link and backscatter link, in which the backscatter link can be seen as an additional transmission path of each PU. What's more, each IoT device with the reflection coefficient is the important node of the backscatter link. The PUs and IoT devices can form multiple PU-IoT pairs. Then, the PU-IoT pairs and BS which further form multiple PU-IoT-BS triples. In each triple, there is one BS, one PU and one IoT device, in which the PU-IoT pair has the cooperative relationship. The cooperative scenario consists of the preferential scenario and the no-preferential scenario. In order to distinguish the two scenarios, we will discuss the two scenarios in Section III and Section IV, respectively.

In the proposed SR-aided IoT networks, each channel consists of two components, which are the small-scale fast fading as well as the large-scale fading component that includes the path loss and shadowing fading. The channel gain from PU m to the BS is denoted as h_m, which equals to $\varepsilon_m^2 l_m$. Furthermore, $h_n = \varepsilon_n^2 l_n$ is the channel gain from IoT Device n to the BS, and the channel gain from PU m to IoT Device n is denoted as $h_{m,n} = \varepsilon_{m,n}^2 l_{m,n}$. In the above equations, ε_m, ε_n, and $\varepsilon_{m,n}$ are small-scale fading components, and l_m, l_n, and $l_{m,n}$ are large-scale fading components.

We assume that the BS accurately knowns the channel state information (CSI) of these links connected to the BS, including the links from PUs and IoT devices to the BS, and the links

from PUs to IoT devices, where the adaptive feedback period scheme [41] is used. In the conceived networks, the users and BS reuse the past CSI as the side information, and the CSI is reported to the BS with a feedback period τ. The large-scale fading components remain unchanged, while the small-scale fading components have a variation for the feedback period τ. We use the first-order Gauss-Markov process and Jakes' model to compute the small-scale fading component over the feedback period τ, which yields

$$\varepsilon(t+\tau) = \xi\varepsilon(t) + e, \tag{1}$$

where $\varepsilon(t)$ and $\varepsilon(t+\tau)$ are the small-scale fading components currently acquired by the BS and the actual small-scale fading component after the feedback period τ respectively, and ξ presents the channel correlation during the feedback period τ. Meanwhile, the channel discrepancy term e is independent of $\varepsilon(t)$, and is distributed according to the complex Gaussian distribution $\mathcal{CN}(0, 1-\xi^2)$ [36], [42].

III. Preferential Scenario

In this section, we firstly present the communication model of the "Preferential Scenario". After that, the cooperative protocol and computing model are introduced. Furthermore, the objective function of maximizing the utility of PUs is formulated.

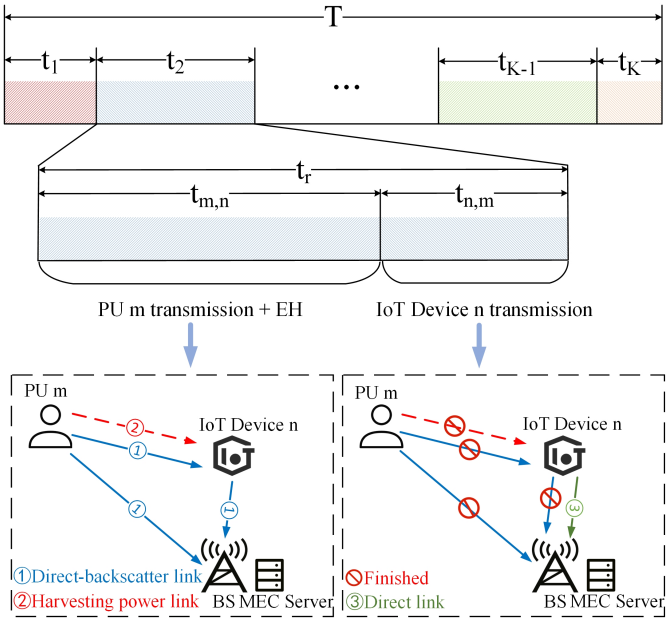

Fig. 2. System model of preferential scenario.

In the "Preferential Scenario", there are two time slots used for the transmission of a PU-IoT pair. The transmission of PU's and IoT device's tasks is in order for the PU-IoT pair in each PU-IoT-BS triple. The "Preferential Scenario" is a win-win scenario for the performances of PUs and IoT devices, where the IoT devices in PU-IoT pairs obtain the transmission power and spectrum resources, and the transmission rates of the matched PUs are improved.

During the first time slot, the offloaded tasks of PU m are transmitted by the direct link and the backscatter link, namely the direct-backscatter link. The IoT Device n is a backscatter device with a backscatter coefficient α_n, which can help the PU m to improve its transmission rate. At the same time, the IoT Device n harvests power from the transmission power provided by the PU m, in which the power harvesting coefficient η_n takes the main part of harvesting power.

During the second time slot, the IoT Device n transmits its offloaded tasks using the harvested power. The transmission rate of PU m is improved under the assistance of the matched IoT Device m. On the other hand, the IoT Device n would pay money to the matched PU m for buying the transmission power with a discount.

A. Communication Model

The tasks to be computed for the PU m and IoT Device n in the conceived SR-aided IoT networks are denoted as D_m and D_n, respectively. For the "Preferential Scenario", the orthogonal multiple access (OMA) technique is used during the PU-IoT pair's transmission period.

As shown in Fig. 2, the required offloading time of PU-IoT pair (m, n), denoted as UP r as well, is given by

$$t_r = t_{m,n} + t_{n,m}, \tag{2}$$

where $t_{m,n}$ and $t_{n,m}$ are the required time for offloading all tasks for the PU m and IoT Device n in this PU-IoT pair. Based on the uplink transmission, the required time for offloading all tasks for the PU m and IoT Device n can be computed by

$$t_{m,n} = \frac{D_m}{R_{m,n}}, \tag{3}$$

and

$$t_{n,m} = \frac{D_n}{R_{n,m}}, \tag{4}$$

respectively, where $R_{m,n}$ and $R_{n,m}$ are the uplink transmission rates for the PU m and IoT Device n. Additionally, the computation ability of MEC server is significantly stronger than the mobile users [43], so the latency of edge computing is small. Thus, compared to the time of uplink offloading and that of local computing, the time of edge computing can be negligible.

Due to the applied OMA technique, there are no interferences between PUs and IoT devices. The messages of each user can be decoded by the BS without any interference. More explicitly, the PUs' messages are decoded firstly by the BS that is integrated with the MEC server. Since the backscatter link is a multi-path component of the direct link. The equivalent channel for decoding the messages of PU m is denoted by

$$h_{eq} = h_m + \alpha_n h_{m,n} h_n, \tag{5}$$

where $\alpha_n \in [0, \frac{1}{2})$ is the backscatter coefficient of IoT Device n, which controls the transmission power of the backscatter link. During the first time slot $t_{m,n}$, the direct-backscatter link

transmission rate $R_{m,n}$ of uplink transmission for the PU m is given by

$$R_{m,n} = B\log_2\left(1+\frac{P_t|h_{eq}|^2}{N_0}\right), \tag{6}$$

where B is the bandwidth of the authorized spectrum, N_0 is the noise power, and P_t is the transmission power.

For the PU m, the transmission power of backscatter link P_b is given by $P_b = \alpha_n P_t|h_{m,n}|^2$. Meanwhile, the IoT Device n can harvest a part of the transmission power P_t to transmit its own tasks by its power harvesting coefficient η_n, equaling to α_n, and the harvested power P_h is given by $P_h = \eta_n P_t|h_{m,n}|^2$. The last part of transmission power P_t, i.e., $(1-\alpha_n-\eta_n)P_t|h_{m,n}|^2$, is used for sustaining the circuit energy consumption. For the IoT Device n, the direct link transmission rate $R_{n,m}$ for uplink transmission in the second time slot $t_{n,m}$ is given by

$$R_{n,m} = B\log_2\left(1+\frac{P_t|h_{m,n}|^2\eta_n|h_n|^2}{N_0}\right). \tag{7}$$

The unit price of power is defined as $a(m)$ per dBm for the PU m. For the IoT Device n with the power harvesting coefficient η_n, the expenditure $EX_{n,m}^{nodis}$ of buying the transmission power from the PU m without any discounts is denoted as

$$EX_{n,m}^{nodis} = P_t|h_{m,n}|^2\eta_n a(m). \tag{8}$$

When the cooperation relationship is not considered, each PU can transmit its own tasks to the MEC server directly. Under this mode, the direct link transmission rate of PU m can be computed by

$$R_m^* = B\log_2\left(1+\frac{P_t|h_m|^2}{N_0}\right). \tag{9}$$

If each IoT device has the available spectrum to transmit its own tasks, the direct link transmission rate of IoT Device n can be computed by

$$R_n^* = B\log_2\left(1+\frac{P_t|h_n|^2}{N_0}\right). \tag{10}$$

Comparing Eq. (6) to Eq. (9), we can conclude that the transmission rate $R_{m,n}$ of PU m is improved for the existing of channel component $\alpha_n|h_{m,n}|^2|h_n|^2$. In particular, for the PU m, the improved rate is denoted as $R_{m,n}^{dif}$, which is given by

$$\begin{aligned} R_{m,n}^{dif} &= R_{m,n} - R_m^* \\ &= B\log_2\frac{1+\rho|h_{eq}|^2}{1+\rho|h_m|^2}, \end{aligned} \tag{11}$$

where ρ equals to $\frac{P_t}{N_0}$. For the improved rate $R_{m,n}^{dif}$, the PU m offers a discount to the IoT Device n who buys its transmission power. The discount is denoted by $b(m)$ per bit per second (bps) for the PU m. Combined with Eq. (8), the income $IN_{m,n}$ of PU m and the actual expenditure $EX_{n,m}$ considering the discount of IoT Devices n are related as

$$\begin{aligned} IN_{m,n} &= EX_{n,m} \\ &= a(m)P_t|h_{m,n}|^2\eta_n - b(m)R_{m,n}^{dif} \\ &= a(m)P_t|h_{m,n}|^2\eta_n - b(m)B\log_2\frac{1+\rho|h_{eq}|^2}{1+\rho|h_m|^2}. \end{aligned} \tag{12}$$

B. Cooperation Protocol

For the tradeoff between the transmission rate and the money, the achievable utilities are set for the PU m and IoT Device n. Considering the direct-backscatter link transmission rate $R_{m,n}$ and income $IN_{m,n}$ of PU m, the achievable utility $\theta_{m,n}$ is given by

$$\begin{aligned} \theta_{m,n} &= \theta_1 R_{m,n} + \theta_2 IN_{m,n} \\ &= \theta_1 R_{m,n} \\ &\quad + \theta_2\left[a(m)P_t|h_{m,n}|^2\eta_n - b(m)B\log_2\frac{1+\rho|h_{eq}|^2}{1+\rho|h_m|^2}\right], \end{aligned} \tag{13}$$

where θ_1 and θ_2 are adjustable factors, satisfying $\theta_1+\theta_2=1$, $\theta_1 \geq 0$, and $\theta_2 \geq 0$. We set φ_1 and φ_2 as adjustable factors as well, which satisfy $\varphi_1+\varphi_2=1$, $\varphi_1 \geq 0$, and $\varphi_2 \geq 0$. Furthermore, φ_1 and φ_2 can be applied to adjust the achievable utility $\varphi_{n,m}$ relating to the direct link transmission rate $R_{n,m}$ and the expenditure $EX_{n,m}$ for IoT Device n, which is formulated as

$$\begin{aligned} \varphi_{n,m} &= \varphi_1 R_{n,m} - \varphi_2 EX_{n,m} \\ &= \varphi_1 R_{n,m} \\ &\quad + \varphi_2\left[b(m)B\log_2\frac{1+\rho|h_{eq}|^2}{1+\rho|h_m|^2} - a(m)P_t|h_{m,n}|^2\eta_n\right]. \end{aligned} \tag{14}$$

Considering the practical utility of users in all matched PU-IoT pairs, the settings of acceptable minimum utility for the PU m and IoT Device n are necessary, which are denoted as θ_m^* and φ_n^* respectively. Based on the direct link transmission rate R_m^* and income $IN_{m,n}$ of PU m, the utility factor θ_m^* is given by

$$\theta_m^* = \theta_1 R_m^* + \theta_2 \mathcal{EV}(IN_m), \tag{15}$$

where IN_m is the summary income of PU m when matching with each IoT device, formulated as

$$\begin{aligned} IN_m &= \sum_{n=1}^{N} IN_{m,n} \\ &= \sum_{n=1}^{N}\left[a(m)P_t|h_{m,n}|^2\eta_n - b(m)B\log_2\frac{1+\rho|h_{eq}|^2}{1+\rho|h_m|^2}\right], \end{aligned} \tag{16}$$

and $\mathcal{EV}(IN_m)$ is the average of the summary income of PU m when matching with each IoT Device, given by

$$\begin{aligned} \mathcal{EV}(IN_m) &= \frac{IN_m}{N} \\ &= \frac{\sum_{n=1}^{N}\left[a(m)P_t|h_{m,n}|^2\eta_n - b(m)B\log_2\frac{1+\rho|h_{eq}|^2}{1+\rho|h_m|^2}\right]}{N}. \end{aligned} \tag{17}$$

Considering the transmission rate and expenditure of the harvested power, the utility factor φ_n^* of IoT Device n can be formulated as

$$\begin{aligned}\varphi_n^* &= \varphi_1 R_n^* - \varphi_2 \mathcal{EV}(EX_n) \\ &= \varphi_1 R_n^* \\ &+ \frac{\varphi_2 \sum\limits_{m=1}^{M} \left[b(m) B \log_2 \frac{1+\rho|h_{eq}|^2}{1+\rho|h_m|^2} - a(m) P_t |h_{m,n}|^2 \eta_n \right]}{N}.\end{aligned} \tag{18}$$

The matching problem of PUs and IoT devices is considered firstly, and they would form R PU-IoT pairs whose set is denoted as $\mathcal{UP} = \{1, 2, \ldots, R\}$. The matching between PUs and IoT devices is a one-to-one matching problem. For any matched results, each user would not have more than one cooperator at the same time, which can be denoted as

$$\mathcal{C}_m \in \{0, 1\}, \text{ and } \mathcal{C}_n \in \{0, 1\}. \tag{19}$$

For $\mathcal{C}_m = 0$, the PU m has failed to form the PU-IoT pair with any IoT device, namely having no cooperators. In addition, $\mathcal{C}_m = 1$ means that the PU m has been matched with a IoT device, i.e. only one IoT device cooperator. So is the IoT Device n. For the matched UP r, the premise of matching is that its achievable utility is not lower than its utility factor. Specifically, the relationships of PU's and IoT device's achievable utility and the respective utility factor satisfy

$$\theta_{m,n} \geq \theta_m^*, \tag{20}$$

and

$$\varphi_{n,m} \geq \varphi_n^*. \tag{21}$$

The BS integrated with the MEC server offers the total transmission duration T, which is divided into K time slots. These time slots have different intervals, which may avoid the high probability that no triples are willing to take the binary offloading mode, and then offer a more flexible time to give more choices to the constructed PU-IoT pairs. The interval of time slot k is denoted as $|t_k|$, which is less than T. In addition, the sum of all time slots satisfies

$$\sum_{k=1}^{K} |t_k| = T. \tag{22}$$

The matching of R PU-IoT pairs and BS is a many-to-one matching problem, where the BS can be used R times. Furthermore, the matching of R PU-IoT pairs and K time slots is a one-to-one matching problem, which can be given by

$$\mathcal{C}_r \in \{0, 1\}, \text{ and } \mathcal{C}_k \in \{0, 1\}. \tag{23}$$

In the obtained triples, there are no repetitive PU-IoT pairs and time slots. For the UP r in the obtained triple (m, n, k), it would not appear in another triple, and the number of its cooperators is 1, denoted as $\mathcal{C}_r = 1$. Meanwhile, for the time slot k in this triple, there is only one cooperator called UP r, and $\mathcal{C}_k$ equals to 1. For those PU-IoT pairs and time slots not in any triples, namely having no cooperators, $\mathcal{C}_r$ and $\mathcal{C}_k$ equal to 0.

For the obtained triple (m, n, k), the offloading mode of UP r depends on the proportion factor ρ_r, which denotes the relationship of the size between t_r and $|t_k|$. Specifically, the proportion factor ρ is formulated as

$$\rho_r = \begin{cases} 1 & \text{Match with BS, } |t_k| \geq t_r, \\ \dfrac{|t_k|}{t_r} & \text{Match with BS, } |t_k| < t_r, \\ 0 & \text{Do not match with BS.} \end{cases} \tag{24}$$

For the UP r matched with the BS, there are two cases: 1) When the interval of the matched time slot k is not less than the required offloading time t_r for the UP r in the triple (m, n, k), the proportion factor ρ_r is 1. The offloading mode applied by this PU-IoT pair is the binary offloading; 2) The proportion factor ρ_r equals to $\frac{|t_k|}{t_r}$, and the UP r applies the partial offloading mode to offload partial tasks, when the interval of the matched time slot k is less than the required offloading time t_r. Meanwhile, the proportion factor ρ_r is 0 for the UP r not matched with the BS. Further, this PU-IoT pair dissolves, and all the tasks of PU m and IoT Device n in this pair are computed by the local servers based on the binary offloading mode. Considering the hybrid offloading mode of PU-IoT pairs, the offloaded tasks D_r for UP r are given by

$$D_r = \begin{cases} D_m + D_n & \text{Match with BS, } |t_k| \geq t_r, \\ \dfrac{|t_k|}{t_r}(D_m + D_n) & \text{Match with BS, } |t_k| < t_r, \\ 0 & \text{Do not match with BS.} \end{cases} \tag{25}$$

For the first and third cases, the binary offloading mode is applied by the UP r. Specifically, the UP r offload all their tasks to the MEC server for the first case, while the UP r dissolves and all the tasks of users in this pair are computed by the local servers for the third case. When the partial offloading mode is applied, the tasks of UP r offloaded to the MEC server are $\frac{|t_k|}{t_r}(D_m + D_n)$, and the remaining tasks of PU m and IoT Device n in this pair are $(1 - \frac{|t_k|}{t_r})D_m$ and $(1 - \frac{|t_k|}{t_r})D_n$, respectively, which are computed by the local servers.

C. Computing Model

In the conceived networks, the servers are divided into two categories, which are local servers and MEC server. The computation capabilities of local servers are limited to compute the corresponding users' tasks. For the local server of PU m, the computation capability is denoted as F_m, which is measured by the frequency of CPUs in the unit of cycles per second or hertz, and is formulated as

$$F_m \geq \frac{D_m f_m}{T}, \tag{26}$$

where f_m is the number of CPU cycles needed by 1 bit data of PU m. Moreover, f_n is treated as the number of CPU cycles needed by 1 bit data of IoT Device n. For the local server of IoT Device n, the computation capability is given by

$$F_n \geq \frac{D_n f_n}{T}. \tag{27}$$

For the MEC server, the computation capability is finite as well, which is denoted as F, measured by the total number of CPU cycles. As a result, the offloaded tasks of PU-IoT pairs in all triples should satisfy the following computation constraint:

$$\sum_{r=1}^{R}(D_m f_m + D_n f_n)\mathcal{C}_r\rho_r \leq F. \tag{28}$$

D. Problem Formulation

As the sellers of communication resource, PUs would consider the benefits of cooperation with the IoT devices. For the sake of balancing the rate and income of PUs, we study the sum-utility maximization problem of PUs matched in the triples, which is formulated as

$$\begin{aligned}\max_{\boldsymbol{\theta_1},\boldsymbol{\varphi_1}} \quad & \sum_{r=1}^{R}\mathcal{C}_r\theta_{m,n} \\ & = \sum_{r=1}^{R}\mathcal{C}_r\Big[\theta_1 R_{m,n} + \theta_2 a(m)P_t|h_{m,n}|^2\eta_n \\ & \quad - \theta_2 b(m)B\log_2\frac{1+\rho|h_{eq}|^2}{1+\rho|h_m|^2}\Big],\end{aligned} \tag{29}$$

$$\begin{aligned} s.t. \quad & (a)\ F_m \geq \frac{D_m f_m}{T},\ F_n \geq \frac{D_n f_n}{T},\ \forall m,\ \forall n, \\ & (b)\ \theta_1 \geq 0,\ \theta_2 \geq 0,\ \theta_1+\theta_2 = 1, \\ & \quad \varphi_1 \geq 0,\ \varphi_2 \geq 0,\ \varphi_1+\varphi_2 = 1, \\ & (c)\ \theta_{m,n} \geq \theta_m^*,\ \varphi_{n,m} \geq \varphi_n^*,\ m,n \in \forall r, \\ & (d)\ \sum_{r=1}^{R}(D_m f_m + D_n f_n)\mathcal{C}_r\rho_r \leq F, \\ & (e)\ \sum_{k=1}^{K}|t_k| = T,\ |t_{k-1}| \neq |t_k| \neq |t_{k+1}|,\ \forall k \in \mathcal{K}_{-2}, \\ & (f)\ \mathcal{C}_m \in \{0,1\},\ \mathcal{C}_n \in \{0,1\},\ \mathcal{C}_r \in \{0,1\}, \\ & \quad \mathcal{C}_k \in \{0,1\},\ \forall m,\ \forall n,\ \forall r,\ \forall k. \end{aligned}$$

Note that (a) guarantees that each local server is able to compute all the tasks of the corresponding users; (b) constrains the relationships between these adjustable factors θ_1, θ_2, φ_1 and φ_2; (c) are the conditions of forming the PU-IoT pair for the PU m and IoT Device n; (d) guarantees all the offloaded tasks can be computed by the MEC server; (e) implies that the total transmission duration T is divided into K time slots with different intervals, where $\mathcal{K}_{-2} = \{2,3,\ldots,K-1\}$; (f) implies that the matching between the PUs and IoT devices is one-to-one, and the matching between the PU-IoT pairs and time slots is.

IV. No-Preferential Scenario

In the "Preferential Scenario", there are two time slots provided for the transmission of each PU-IoT pair. More explicitly, the first time slot is for the transmission of the PU m as well as the process of harvesting power for the IoT Device n. In addition, the second time slot is for the IoT Device n to upload its tasks to the BS after the transmission of the matched PU m, aiming to obtain a discount of improving the transmission rate of this PU m. Unlike the "Preferential Scenario", in the "No-Preferential Scenario", there is only one time slot provided for each PU-IoT pair, where the PU m and IoT Device n upload their offloaded tasks to the BS simultaneously, and there is no discount for the IoT Device n due to its interference to the PU m. Without considering the monetary transactions, the "No-Preferential Scenario" is a single-win scenario, where IoT devices in PU-IoT pairs obtain the transmission power and spectrum resources, but the transmission rates of these matched PUs are negatively affected.

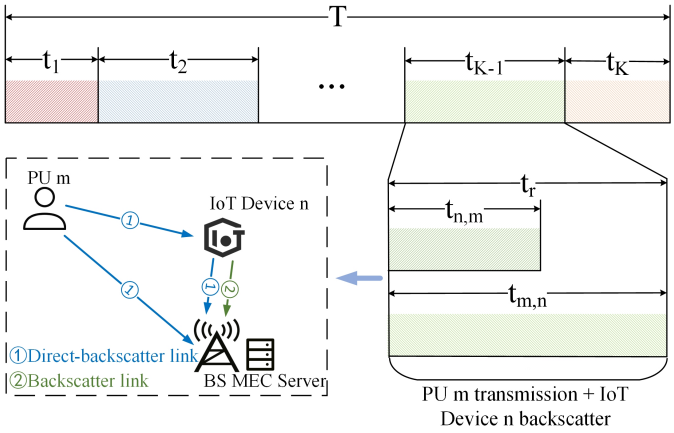

Fig. 3. System model of no-preferential scenario.

Specifically, the PU m in the UP r uploads its tasks to the BS by the direct-backscatter link. Meanwhile, the IoT Device n in this pair uploads the offloaded tasks to the BS by the transmission power obtained with the backscatter coefficient α_n. Explicitly, the process of harvesting power based on the power harvesting coefficient η_n is not needed. Furthermore, the BS integrated with a MEC server applies the successive interference cancellation (SIC) technique to decode the received messages. At the BS, the messages of PU m are firstly decoded under the interference from the matched IoT Device m, then only the messages of IoT Device n are decoded. The direct-backscatter link transmission rate of PU m is influenced by the transmission of the IoT Device n. Hence, this IoT Device n would suffer from a higher expenditure for buying the transmission power from the matched PU m without a discount.

A. Communication Model

The NOMA technique is applied to improve spectral efficiency and user fairness [44], [45]. The PU m and IoT Device n in the UP r upload their tasks simultaneously. The required offloading time of UP r is denoted as

$$t_r = \max\{t_{m,n}, t_{n,m}\}, \tag{30}$$

which is the longer time among the required offloading time of PU m and IoT Device n in this pair, as shown in Fig. 3, which aims to guarantee that each user has the authority to offload

all the tasks. Additionally, the required offloading time of PU m and IoT Device n are determined, respectively, as

$$t_{m,n} = \frac{D_m}{R_{m,n}}, \tag{31}$$

and

$$t_{n,m} = \frac{D_n}{R_{n,m}}, \tag{32}$$

where $R_{m,n}$ and $R_{n,m}$ are the rates of uplink transmission for the PU m and IoT Device n. At the BS, the SIC technique is applied to decode the messages of users, where the messages of PU m in the UP r is decoded firstly.

In the conceived networks, the bandwidth of the authorized spectrum is denoted as B, the noise power is denoted as N_0, and the transmission power is denoted as P_t. The direct-backscatter link transmission rate of the PU m in the UP r is given by

$$R_{m,n} = B\log_2\left[1 + \frac{P_t(|h_m|^2 + \alpha_n|h_{m,n}|^2|h_n|^2)}{N_0 + P_t|h_{m,n}|^2\alpha_n|h_n|^2}\right], \tag{33}$$

where $\alpha_n \in [0, \frac{1}{2})$ is the backscatter coefficient of IoT Device n controlling the transmission power of backscatter link, and the transmission power of backscatter link for the PU m and IoT Device n in this pair is given by $P_b = \alpha_n P_t|h_{m,n}|^2$.

The direct-backscatter link transmission rate $R_{m,n}$ of PU m is influenced by the matched IoT Device n, and the direct link transmission rate R_m^* is given by

$$R_m^* = \beta B\log_2\left(1 + \frac{P_t|h_m|^2}{N_0}\right), \tag{34}$$

where β is the rate regulation factor, and $\beta \in (0, 1]$. The messages of the matched IoT Device n are decoded secondly, and the backscatter link transmission rate of IoT Device n is given by

$$R_{n,m} = B\log_2\left(1 + \frac{P_t|h_{m,n}|^2\alpha_n|h_n|^2}{N_0}\right), \tag{35}$$

where the transmission power is bought from the matched PU m by the unit price $a(m)$ per dBm. Furthermore, the expenditure $EX_{n,m}$ of IoT Device n is determined by

$$EX_{n,m} = P_t|h_{m,n}|^2\alpha_n a(m). \tag{36}$$

For the "Preferential Scenario", the transmission power of IoT Device n in the UP r is harvested from the matched PU m by the power harvesting coefficient η_n during the first time slot, and then the IoT Device n uploads tasks using the harvested power during the second time slot, so the expenditure $EX_{n,m}$ is relating to the power harvesting coefficient η_n. Differently, for the "No-Preferential Scenario", there is only one time slot for each PU-IoT pair, and no process of the IoT device n harvesting the power from the matched PU m. The PU and IoT device in each PU-IoT pair upload the offloaded tasks to the BS simultaneously, and the transmission power of IoT device n is determined by the backscatter coefficient α_n, which is relating to the expenditure $EX_{n,m}$ of IoT Device n as well.

No discounts are provided to the IoT Device n in the UP r, since the transmission rate of the matched PU m decreases by the interference of IoT Device n. For the "No-Preferential Scenario", the income $IN_{m,n}$ is equal to the expenditure $EX_{n,m}$ of IoT Device n, given by

$$\begin{aligned} IN_{m,n} &= EX_{n,m} \\ &= a(m)P_t|h_{m,n}|^2\alpha_n. \end{aligned} \tag{37}$$

B. Cooperation Protocol

As the seller, each PU needs to weight the transmission rate and income. The utility factor θ_m^* is the acceptable minimum utility of PU m, which is relating to the direct link transmission rate R_m^* and the average $\mathcal{EV}(IN_m)$ of the total income of PU m matching with each IoT device, given by

$$\begin{aligned} \theta_m^* &= \theta_1 R_m^* + \theta_2\mathcal{EV}(IN_m) \\ &= \theta_1 R_m^* + \frac{\theta_2\sum_{n=1}^{N} IN_{m,n}}{N} \\ &= \theta_1 R_m^* + \frac{\theta_2\sum_{n=1}^{N} a(m)P_t|h_{m,n}|^2\alpha_n}{N}, \end{aligned} \tag{38}$$

where θ_1 and θ_2 are positive adjustable factors, and satisfy $\theta_1+\theta_2 = 1$. The utility factor θ_m^* is the measure of whether the matching between the PU m and each IoT device is acceptable. The practical utility of the PU m matching with the IoT Device n, called achievable utility $\theta_{m,n}$, is formulated as

$$\begin{aligned} \theta_{m,n} &= \theta_1 R_{m,n} + \theta_2 IN_{m,n} \\ &= \theta_1 R_{m,n} + \theta_2 a(m)P_t|h_{m,n}|^2\alpha_n. \end{aligned} \tag{39}$$

As the consumer, each IoT device needs to weight the transmission rate and the expenditure as well. If each IoT device has the available spectrum to transmit its tasks, the direct link transmission rate R_n^* of IoT Device n can be computed by

$$R_n^* = B\log_2\left(1 + \frac{P_t|h_n|^2}{N_0}\right). \tag{40}$$

Considering the direct link transmission rate R_n^* and the average expenditure EX_n, the utility factor φ_n^* of IoT Device n is denoted as

$$\begin{aligned} \varphi_n^* &= \varphi_1 R_n^* - \varphi_2\mathcal{EV}(EX_n) \\ &= \varphi_1 R_n^* - \frac{\varphi_2\sum_{m=1}^{M} P_t|h_{m,n}|^2\alpha_n a(m)}{M}, \end{aligned} \tag{41}$$

where φ_1 and φ_2 are positive adjustable factors, and satisfy $\varphi_1 + \varphi_2 = 1$ as well. For the IoT Device n matching with the PU m, the achievable utility $\varphi_{n,m}$ is given by

$$\begin{aligned} \varphi_{n,m} &= \varphi_1 R_{n,m} - \varphi_2 EX_{n,m} \\ &= \varphi_1 R_{n,m} - \varphi_2 P_t|h_{m,n}|^2\alpha_n a(m). \end{aligned} \tag{42}$$

The matching between the PUs and IoT devices is one-to-one matching problem, denoted as

$$\mathcal{C}_m \in \{0, 1\}, \text{ and } \mathcal{C}_n \in \{0, 1\}. \tag{43}$$

For each obtained UP r, the achievable utilities of the PU m and IoT Device n are not lower than their utility factors, formulated as

$$\theta_{m,n} \geq \theta_m^*, \tag{44}$$

and

$$\varphi_{n,m} \geq \varphi_n^*. \tag{45}$$

Furthermore, the matching between the K time slots of BS and the PU-IoT pairs is one-to-one matching as well, which is formulated as

$$\mathcal{C}_r \in \{0,1\}, \text{ and } \mathcal{C}_k \in \{0,1\}. \tag{46}$$

The offloading mode and offloaded tasks of the PU-IoT pair in the obtained triple (m,n,k) are related to the proportion factor ρ_r, which is given by

$$\rho_r = \begin{cases} 1 & \text{Match with BS, } |t_k| \geq t_r, \\ \dfrac{|t_k|}{t_r} & \text{Match with BS, } |t_k| < t_r, \\ 0 & \text{Do not match with BS,} \end{cases} \tag{47}$$

where $\rho_r = 1$ denotes that the UP r would offload all the tasks to the BS during the matched time slot k by the binary offloading mode. When ρ_r equals to $\frac{|t_k|}{t_r}$, the UP r applies the partial offloading mode to offload partial tasks. Otherwise, the proportion factor ρ_r is 0 for the UP r not matched with the BS. Further, this PU-IoT pair dissolves, and all the tasks of PU m and IoT Device n in this pair are computed by the local servers based on the binary offloading mode. The sizes of tasks for each user with different ρ_r are computed by

$$D_r = \begin{cases} D_m + D_n & \text{Match with BS, } |t_k| \geq t_r, \\ \dfrac{|t_k|}{t_r}(D_m + D_n) & \text{Match with BS, } |t_k| < t_r, \\ 0 & \text{Do not match with BS.} \end{cases} \tag{48}$$

C. Computing Model

The computation capabilities of local servers and MEC server are finite, the computation capability of PU m's local server is given by

$$F_m \geq \frac{D_m f_m}{T}, \tag{49}$$

where f_m is the number of CPU cycles needed by 1 bit data of PU m. The number of CPU cycles needed by 1 bit data of IoT Device n is denoted as f_n, and the computation capability of IoT Device n's local server is formulated as

$$F_n \geq \frac{D_n f_n}{T}. \tag{50}$$

We treat F as the total number of CPU cycles for the MEC server, and F satisfies

$$\sum_{r=1}^{R} (D_m f_m + D_m f_n)\mathcal{C}_r \rho_r \leq F. \tag{51}$$

D. Problem Formulation

Considering the utility of PUs in all the final triples, the sum-utility maximization problem can be formulated as

$$\begin{aligned} \max_{\boldsymbol{\theta_1}, \boldsymbol{\varphi_1}, \boldsymbol{\beta}} \quad & \sum_{r=1}^{R} \mathcal{C}_r \theta_{m,n} \\ & = \sum_{r=1}^{R} \mathcal{C}_r \left[\theta_1 R_{m,n} + \theta_2 a(m) P_t |h_{m,n}|^2 \alpha_n\right], \end{aligned} \tag{52}$$

$$\begin{aligned} s.t. \quad & (a)\ F_m \geq \frac{D_m f_m}{T},\ F_n \geq \frac{D_n f_n}{T},\ \forall m,\ \forall n, \\ & (b)\ \theta_1 \geq 0,\ \theta_2 \geq 0,\ \theta_1 + \theta_2 = 1, \\ & \quad \varphi_1 \geq 0,\ \varphi_2 \geq 0,\ \varphi_1 + \varphi_2 = 1, \\ & \quad 0 < \beta \leq 1, \\ & (c)\ \theta_{m,n} \geq \theta_m^*,\ \varphi_{n,m} \geq \varphi_n^*,\ m,n \in \forall r, \\ & (d)\ \sum_{r=1}^{R} (D_m f_m + D_n f_n)\mathcal{C}_r \rho_r \leq F, \\ & (e)\ \sum_{k=1}^{K} |t_k| = T,\ |t_{k-1}| \neq |t_k| \neq |t_{k+1}|,\ \forall k \in \mathcal{K}_{-2}, \\ & (f)\ \mathcal{C}_m \in \{0,1\},\ \mathcal{C}_n \in \{0,1\},\ \mathcal{C}_r \in \{0,1\}, \\ & \quad \mathcal{C}_k \in \{0,1\},\ \forall m,\ \forall n,\ \forall r,\ \forall k. \end{aligned}$$

Note that (a) guarantees that each local server is able to compute all the tasks of the corresponding users; (b) constrains the relationships between these adjustable factors θ_1, θ_2, φ_1 and φ_2, and gives the range of rate regulation factor β; (c) are the conditions of forming the PU-IoT pair for the PU m and IoT Device n; (d) guarantees that all the offloaded tasks can be computed by the MEC server; (e) implies that the total transmission duration T is divided into K time slots with different intervals, where $\mathcal{K}_{-2} = \{2,3,\ldots,K-1\}$; (f) implies that the matching between the PUs and IoT devices is one-to-one, and the matching between the PU-IoT pairs and time slots is.

V. Utility Based Resources Sharing Algorithm

Now we study the resources sharing scheme considering the monetary transactions, including the power, spectrum, time, and server resources. In Section III and IV, we have proposed two scenarios relating to the relationships between the PUs and IoT devices. In the "Preferential Scenario", the relationships between the users in the triples are win-win, where the transmission rates of PUs are improved by the assistance of the matched IoT devices, and the IoT devices could transmit tasks using the obtained transmission power and spectrum resources with a discounted price. Specifically, the processes of offloading tasks for the users in each triple are in order, where PUs go firstly. The PUs in the triples charge the matched IoT devices for the shared transmission power, where the discounts relating to the assistance of IoT devices are considered. In the "No-Preferential Scenario", the relationships between the users in the triples are single win, where the IoT devices obtain the transmission power and

spectrum resources, and the transmission rates of PUs are interfered by the matched IoT devices. In detail, the users in the triples upload tasks at the same time, and the PUs charge the matched IoT devices for the shared power without any discounts.

The resources sharing problem is a three-sided matching problem for the PUs, IoT devices and BS. The three-sided matching problem is NP-hard [46], [47], and there are no polynomial-complexity algorithms to find the optimal solutions of Eq. (29) and Eq. (52). To obtain the approximate solutions, we propose the utility based resources sharing algorithm to solve the three-sided matching problems in the conceived networks, which is shown in **Algorithm 1**. In detail, we dissolve the resources sharing problem into two subproblems, which are the power and spectrum sharing between the PUs and IoT devices, as well as the time and servers sharing between the PU-IoT pairs and BS.

Algorithm 1: Utility Based Resources Sharing Algorithm

Step 1: *Initialize*

1) Adjustable factors θ_1, θ_2, φ_1 and φ_2;
2) Utility factors θ_m^* and φ_n^*;

Step 2: *Match the PUs and IoT devices*

Repeat

1) Update the preference list $\boldsymbol{PL}_{M\times N}$;
2) PUs without cooperators send the matching invitations to the most anticipated IoT device;
3) **If** the IoT device has no cooperator **then**
4) $\varphi_{n,m} \geq \varphi_n^* \Rightarrow (m,n)$;
   $\varphi_{n,m} < \varphi_n^* \Rightarrow$remain single;
5) **Else if** it has a cooperator PU m_{ex} **then**
6) $\varphi_{n,m} > \varphi_{n,m_{ex}} \Rightarrow (m,n)$;
   $\varphi_{n,m} \leq \varphi_{n,m_{ex}} \Rightarrow (m_{ex},n)$;
7) **End if**

Until $\boldsymbol{PL}_m|_{\text{single PU } m}=\boldsymbol{O}$

Step 3: *Determine the offloading strategy of PU-IoT pairs*

Compute the offloading time of all PU-IoT pairs;

Repeat

1) Update the preference list $\boldsymbol{PL}_{R\times K}$;
2) UPs without scheduling send the matching invitations to the BS for the most anticipated time slot;
3) **If** the time slot has not been scheduled **then**
4) $(m,n,k) \Rightarrow \rho_r$;
5) **Else if** it has been scheduled with the UP r_{ex}, and the proportion factor $\rho_{r_{ex}}$ is known **then**
6) $\rho_r = 1,\ \rho_{r_{ex}} < 1 \Rightarrow (m,n,k)$;
   $\rho_r < 1,\ \rho_{r_{ex}} = 1 \Rightarrow (m_{ex},n_{ex},k)$;
   $\rho_{r_{ex}} < \rho_r < 1 \Rightarrow (m,n,k)$;
   $\rho_r \leq \rho_{r_{ex}} < 1 \Rightarrow (m_{ex},n_{ex},k)$;
   $\rho_r = \rho_{r_{ex}} = 1, t_{r_{ex}} < t_r \Rightarrow (m,n,k)$;
   $\rho_r = \rho_{r_{ex}} = 1, t_{r_{ex}} \geq t_r \Rightarrow (m_{ex},n_{ex},k)$;
7) **End if**

Until $\boldsymbol{PL}_r|_{\text{single UP } r}=\boldsymbol{O}$

A. Power and Spectrum Resources Sharing Scheme

For both scenarios, the processes of matching between the PUs and IoT devices are one-to-one matching, and each user would like to maximize its own utility, denoted as Eq. (13), Eq. (14), Eq. (39) and Eq. (42). Furthermore, the PUs are the providers of the transmission power and spectrum resources, and have the authorities and priorities to choose the IoT devices that they would like to cooperate with. For each PU, the utility brought by each IoT device is different, which decides the priorities of the PU's selections among all the IoT devices. For the IoT devices satisfying Eq. (20) and Eq. (44) of the PU m, the set is denoted as

$$PL_m^{ZF} = \{n \mid \ \theta_{m,n} \geq \theta_m^*\}, \tag{53}$$

and the elements of PL_m^{ZF} form the zero-free preference list $\boldsymbol{PL}_m^{ZF}$ in the following order:

$$\theta_{m,\boldsymbol{PL}_m^{ZF}(1)} \geq \theta_{m,\boldsymbol{PL}_m^{ZF}(2)} \geq \cdots \geq \theta_{m,\boldsymbol{PL}_m^{ZF}(N_m^*)}, \tag{54}$$

where N_m^* is the number of elements of the $\boldsymbol{PL}_m^{ZF}$.

In addition, considering the IoT devices not satisfying Eq. (20) and Eq. (44) of the PU m, they are denoted as 0 in the complete preference list $\boldsymbol{PL}_m$ of the PU m, and the complete preference list $\boldsymbol{PL}_m$ of the PU m is determined as

$$\boldsymbol{PL}_m = [\boldsymbol{PL}_m^{ZF}, \boldsymbol{O}_{N-N_m^*}], \tag{55}$$

where $\boldsymbol{O}_{N-N_m^*}$ is the the zero vector with the length $N-N_m^*$. The complete preference lists of all the PUs are different, and they form the preference list $\boldsymbol{PL}_{M\times N}$ of M PUs in parallel, which is denoted as

$$\boldsymbol{PL}_{M\times N} = \begin{bmatrix} \boldsymbol{PL}_1^{ZF}, \boldsymbol{O}_{N-N_1^*} \\ \boldsymbol{PL}_2^{ZF}, \boldsymbol{O}_{N-N_2^*} \\ \vdots \\ \boldsymbol{PL}_m^{ZF}, \boldsymbol{O}_{N-N_m^*} \\ \vdots \\ \boldsymbol{PL}_M^{ZF}, \boldsymbol{O}_{N-N_M^*} \end{bmatrix}. \tag{56}$$

Based on the preference list $\boldsymbol{PL}_{M\times N}$, each PU who has not been matched with others sends the matching invitation to the respective best choice located at the first location of the corresponding row in the $\boldsymbol{PL}_{M\times N}$. Meanwhile, the invited IoT devices have two cases, which are single or not single. No matter which the case is, there may be more than one PU sending the matching invitations to the same IoT device, and it's just a matter of who sends the invitation firstly.

For the invited IoT Device n without a cooperator, if the achievable utility $\varphi_{n,m}$ brought by the PU m is not lower than its utility factor φ_n^*, the IoT Device n accepts the invitation of PU m, and the PU-IoT pair (m,n) is obtained. Otherwise, the IoT Device n rejects the invitation of PU m and remains single. For the invited IoT Device m matched with the PU m_{ex}, if the achievable utility $\varphi_{n,m}$ brought by the PU m is higher than the achievable utility $\varphi_{n,m_{ex}}$ brought by the PU m_{ex}, the IoT Device n accepts the invitation of PU m and abandons the PU m_{ex}, the PU-IoT pair (m,n) is obtained. Otherwise, the IoT Device n rejects the invitation of PU m and keeps the PU-IoT pair (m_{ex},n) with the PU m_{ex}.

After the above processes, the PU m which is rejected or abandoned by the IoT Device n updates its zero-free preference list $\boldsymbol{PL}_m^{ZF}$, by treating the utility brought by the the IoT Device n as 0 and removing the IoT Device n from the $\boldsymbol{PL}_m^{ZF}$. Considering all the rejected or abandoned PUs, the preference list $\boldsymbol{PL}_{M\times N}$ is updated. Based on the updated $\boldsymbol{PL}_{M\times N}$, the matching of the PUs without the cooperators and IoT devices begins again. The above processes are repeated until the complete preference list $\boldsymbol{PL}_m$ of each PU without a cooperator becomes a zero vector $\boldsymbol{O}$, and R PU-IoT pairs, which would share the power and spectrum resources, are obtained.

B. Time and Servers Resources Sharing Scheme

All PU-IoT pairs need to solve the issue on the number of tasks, which server to use and the time to operate. In the conceived networks, there is only one BS integrated with the MEC server that can compute the offloaded tasks. Moreover, the matching between the PU-IoT pairs and BS is a many-to-one matching. For the sake of satisfying the offloading requirements of all the PU-IoT pairs, the total transmission duration T is divided into many time slots, while the matching between the PU-IoT pairs and time slots is a one-to-one matching. Based on the Eq. (2) and Eq. (30), the required offloading time can be computed. The required offloading time of R PU-IoT pairs are different, since the tasks and transmission rates of all the users are different. The total transmission duration T is divided into K time slots with different intervals, in order to provide different solutions to the PU-IoT pairs with the different offloading time.

Faced with K different time slots, there are two offloading modes for each PU-IoT pair, which are the binary and partial offloading modes. Each PU-IoT pair would like to offload tasks by the binary mode, and the set of the time slots that allow the UP r to offload tasks by the binary mode is denoted as

$$PL_r^{BM} = \{k \mid \ |t_k| \geq t_r\}, \tag{57}$$

where K_r^{BM} elements form the binary-mode preference list $\boldsymbol{PL}_r^{BM}$ in the following order:

$$|t_{\boldsymbol{PL}_r^{BM}(1)}| \leq |t_{\boldsymbol{PL}_r^{BM}(2)}| \leq \cdots \leq |t_{\boldsymbol{PL}_r^{BM}(K_r^{BM})}|. \tag{58}$$

The remaining time slots only allow the UP r to offload tasks by the partial mode, and the set of these time slots is denoted as

$$PL_r^{PM} = \{k \mid \ t_r > |t_k|, \text{ and } |t_k| \neq 0\}, \tag{59}$$

where the number of elements are denoted as K_r^{PM}, and the elements form the partial-mode preference list $\boldsymbol{PL}_r^{PM}$ in the following order:

$$|t_{\boldsymbol{PL}_r^{PM}(1)}| \geq |t_{\boldsymbol{PL}_r^{PM}(2)}| \geq \cdots \geq |t_{\boldsymbol{PL}_r^{PM}(K_r^{PM})}|. \tag{60}$$

There may be some time slots whose intervals are zero, and cannot be used by the PU-IoT pairs. In the complete preference list $\boldsymbol{PL}_r$ of UP r, the time slots that cannot be used are denoted 0. The $\boldsymbol{PL}_r$ is formulated as

$$\boldsymbol{PL}_r = [\boldsymbol{PL}_r^{BM}, \boldsymbol{PL}_r^{PM}, \boldsymbol{O}_{K-K_r^{BM}-K_r^{PM}}], \tag{61}$$

where $\boldsymbol{O}_{K-K_r^{BM}-K_r^{PM}}$ is the zero vector with the length $K - K_r^{BM} - K_r^{PM}$.

Arranging the complete preference lists of all the PU-IoT pairs in parallel, the preference list $\boldsymbol{PL}_{R\times K}$ is given by

$$\boldsymbol{PL}_{R\times K} = \begin{bmatrix} \boldsymbol{PL}_1^{BM}, \boldsymbol{PL}_1^{PM}, \boldsymbol{O}_{K-K_1^{BM}-K_1^{PM}} \\ \boldsymbol{PL}_2^{BM}, \boldsymbol{PL}_2^{PM}, \boldsymbol{O}_{K-K_2^{BM}-K_2^{PM}} \\ \vdots \\ \boldsymbol{PL}_r^{BM}, \boldsymbol{PL}_r^{PM}, \boldsymbol{O}_{K-K_r^{BM}-K_r^{PM}} \\ \vdots \\ \boldsymbol{PL}_R^{BM}, \boldsymbol{PL}_R^{PM}, \boldsymbol{O}_{K-K_R^{BM}-K_R^{PM}} \end{bmatrix}. \tag{62}$$

According to the preference list $\boldsymbol{PL}_{R\times K}$, each PU-IoT pair that is not matching with any time slots would send the matching invitation to the BS for matching with the respective first choice. If the invited time slot has not been matched with other PU-IoT pairs, the time slot would accept the invitation, and forms the triple (m, n, k) with the UP r. Meanwhile, the proportion factor ρ_r is given by Eq. (24) and Eq. (47).

If the invited time slot has been matched with a PU-IoT pair denoted as UP r_{ex}, then the proportion factor ρ_r of the inviting UP r would be computed firstly. Then there are a few cases need to be considered. For $\rho_r = 1$ and $\rho_{r_{ex}} < 1$, the PU-IoT pair who could offload tasks by the binary mode is the first choice for the invited time slot k, and the time slot k accepts the invitation of UP r and abandons the UP r_{ex}, forming the triple (m, n, k). For $\rho_r < 1$ and $\rho_{r_{ex}} = 1$, the UP r_{ex} that could take the binary offloading mode is selected by the invited time slot k, and the inviting UP r is rejected.

For $\rho_r < 1$ and $\rho_{r_{ex}} < 1$, if the proportion factor $\rho_{r_{ex}}$ is lower than the ρ_r, the invited time slot k accepts the invitation of UP r, which has the bigger proportion factor to offload more of its tasks. Otherwise, the UP r is rejected by the invited time slot k, and the triple (m_{ex}, n_{ex}, k) matching with the UP r_{ex} is kept. For $\rho_r = \rho_{r_{ex}} = 1$, the invited time slot k would select the PU-IoT pair having the longer offloading time, in order to reduce the time wasters. In detail, if the offloading time of UP r is higher than that of the UP r_{ex}, the invited time slot k accepts the invitation of UP r, and forms the triple (m, n, k). Otherwise, the triple (m_{ex}, n_{ex}, k) matching with the UP r_{ex} is kept.

After the above processes, the UP r rejected or abandoned by the time slot k would not send the matching invitation to it again, and treats the interval of this time slot as 0. Considering all the rejected or abandoned PU-IoT pairs, the preference list $\boldsymbol{PL}_{R\times K}$ is updated. Furthermore, the matching between the PU-IoT pairs and BS starts again. The processes of matching and updating are repeated until the complete preference list $\boldsymbol{PL}_r$ of each PU-IoT pair without matching with the BS equals to the zero vector $\boldsymbol{O}$.

C. Resources Sharing Scheme, Stability and Complexity

1) Resources Sharing Scheme: Based on the proposed algorithm, the problem of resources sharing in the "Preferential Scenario" and "No-Preferential Scenario" could be solved.

Specifically, R triples can be obtained using the utility based resources sharing algorithm.

For the triple (m, n, k) in the "Preferential Scenario", the PU m firstly offloads tasks to the MEC server based on the proportion factor ρ_r via the direct-backscatter link. Meanwhile, the IoT Device n in the backscatter link harvests the power from the PU m depending on the power harvesting coefficient η_n, and then offloads tasks to the MEC server depending on the proportion factor ρ_r by employing the harvested power. More specifically, the IoT Device n pays PU m for the harvested power by subtracting the discount of extra improving its transmission rate, and the extra improved transmission rate is the difference of the direct-backscatter link transmission rate and the direct link transmission rate.

For the triple (m, n, k) in the "No-Preferential Scenario", the PU m and IoT Device n offload their tasks to the MEC server depending on the proportion factor ρ_r simultaneously, which the IoT Device n obtains the transmission power from the PU m depending on the backscatter coefficient α_n, and has effect on the transmission rate of PU m. In particular, the IoT Device n pays the PU m for the obtained transmission power without any discount.

For users who have not matched with others, their tasks are computed by the local servers.

2) Stability: For a stable two-sided matching, there will be no destabilizing pairs [48]. If the PU m^* and IoT Device n^* have been matched with other users under the current matching results, but they prefer each other than the current cooperators, then, the destabilizing pair (m^*, n^*) is formed between them, and the matching is not stable.

The proposed three-sided matching problem for the PUs, IoT devices and BS is in fact a two two-sided matching problem, which is the matching between the PUs and IoT devices, and the matching between the PU-IoT pairs and BS. More specifically, the utility based resources sharing algorithm is a two-step two-sided matching algorithm. The stability of the proposed algorithm is analyzed as follows.

We assume that there is a triple (m^*, n^*, k^*) not included in the current matching results, and this triple is divided into two pairs (m^*, n^*) and (r^*, k^*). For the PU-IoT pair (m^*, n^*), two cases are considered. If the PU m^* has not sent the matching invitation to the IoT Device n^*, there are two reasons: 1) the IoT Device n^* is not in the complete preference list $\boldsymbol{PL}_m$ of PU m^*; 2) the PU m^* has matched with another better cooperator. If the PU m^* has sent the matching invitation to the IoT Device n^*, the reasons that it has been rejected are: 1) the requirement of the IoT Device n^* could not be satisfied by the PU m^*; 2) the IoT Device n^* has matched with another better cooperator. Hence, we could conclude that the PU m^* and IoT Device n^* do not prefer each other than the current cooperators, and the PU-IoT pair (m^*, n^*) is not a destabilizing pair.

For the pair (r^*, k^*), two cases are considered as well. If the UP r^* has not sent the matching invitation to the time slot k^*, there are two reasons: 1) the interval of time slot k^* is 0, and it is not in the complete preference list $\boldsymbol{PL}_r$ of UP r^*; 2) the UP r^* has matched with another better cooperator. If the UP r^* has sent the matching invitation to the time slot k^*, then the reason that the UP r^* has been rejected, is that the time slot k^* has matched with another better cooperator. Therefor, we could conclude that the pair (r^*, k^*) is not a destabilizing pair, and the triple (m^*, n^*, k^*) is not a destabilizing triple. Hence, there are no destabilizing triples for the current matching results, and the stability of the proposed algorithm is proved.

3) Complexity: In the communication phase, during the matching process of the PUs and IoT devices, each PU sends the invitation to the first choice of its preference list in each round. The worst case is that each PU may send their invitations to IoT devices for N times. For M PUs, the complexity can be computed as $O(MN)$.

After the matching process of the PUs and IoT devices is finished, M PU-IoT pairs could be obtained at most. For M PU-IoT pairs, they would like to match with the BS in the computing phase. During this process, each user pair would sent the matching invitation to the BS for K times at most. For M PU-IoT pairs, the complexity is given by $O(MK)$. Combing above two processes, the complexity of the proposed algorithm can be expressed as

$$O(MN + MK) = O(2M^2). \tag{63}$$

VI. Simulation Results

In this section, the simulation results are presented to evaluate the performances of the proposed algorithm in the "Preferential Scenario" and "No-Preferential Scenario". Then, in order to highlight the superiority of the proposed algorithm, the centralized algorithm and random algorithm are considered for comparison.

A. Simulation Setup

In this paper, the channel gain is denoted by $h = \varepsilon^2 l$, where ε is the small-scale fading component, l is the large-scale fading component. For both the "Preferential Scenario" and "No-Preferential Scenario", the distances between the PUs and BS are not more than 25 meters, and the distances between the IoT devices and BS are not more than 20 meters. The other parameters are set as follows. The bandwidth of the authorized spectrum is $B = 10$ MHz, the noise power is $N_0 = -30$ dBm, and $P_t = 25$ dBm is the transmission power. In addition, the computation capability of MEC server is $F = 4 \times 10^{11}$ cycles/s. For the IoT Device n, the task size, the required number of CPU cycles per bit and the computation capability are $D_n \in (0, 30]$ Mbit, $f_n \in [50, 100]$ cycles/bit and $F_n = 200$ MHz, respectively. Meanwhile, the backscatter coefficient and the power harvesting coefficient of IoT Device n are $\eta_n = \alpha_n \in [0, \frac{1}{2})$. For the PU m, the task size, the required number of CPU cycles per bit and the computation capability are $D_m \in (0, 40]$ Mbit, $f_m \in [50, 100]$ cycles/bit and $F_m = 300$ MHz, respectively. The local computation energy per cycle for each user is set as $P_m = P_n = 0.5$ J/cycle. Considering the money transactions, the unit price of selling power for the PU m is $a(m) \in [0.2, 0.3]$ \$/dBm, and

the preferential price of the improved transmission rate given by the PU m is $b(m) \in [0.1, 0.2]$ \$/dBm.

B. Performance Analysis

According to Eq. (29) and Eq. (52), the utility of PUs is relating to the utility factors θ_m^* and φ_n^*, where the adjustable factors θ_1, θ_2, φ_1 and φ_2 determine the proportion of the transmission rates and income, and then influence the utility of all the PUs. The proposed algorithm is to maximize the utility of all the PUs based on the established adjustable factors, instead of maximizing the utility of all the PUs by adjusting the adjustable factors. Specifically, there are three main cases for the adjustable factors θ_1 and θ_2, which are shown as follows:

- $\theta_1 > \theta_2$, PUs prefer the transmission rates;
  - $\theta_1 = 1,\ \theta_2 = 0$, only rates are considered;
- $\theta_1 < \theta_2$, PUs prefer the income;
  - $\theta_1 = 0,\ \theta_2 = 1$, only income is considered;
- $\theta_1 = \theta_2$, the transmission rates and income have the same proportion for the PUs.

Meanwhile, for the adjustable factors φ_1 and φ_2, we have the following cases:

- $\varphi_1 > \varphi_2$, IoT devices prefer the obtained transmission power;
  - $\varphi_1 = 1,\ \varphi_2 = 0$, only power is considered;
- $\varphi_1 < \varphi_2$, IoT devices prefer the expenditure;
  - $\varphi_1 = 0,\ \varphi_1 = 1$, only expenditure is considered;
- $\varphi_1 = \varphi_2$, the obtained transmission power and expenditure have the same proportion for the IoT devices.

As shown in Fig. 4, the approximate solutions of Eq. (29) and Eq. (52) relating to different adjustable factors are obtained by the proposed algorithm in the "Preferential Scenario" and "No-Preferential Scenario". Fig. 4(a) shows the approximate solutions in terms of the 'Utility' based on the established different adjustable factors 'θ_1' and 'φ_1' for the "Preferential Scenario", while Fig. 4(b) shows that of the "No-Preferential Scenario", where $\theta_2 = 1 - \theta_1$, and $\varphi_2 = 1 - \varphi_1$. No matter what the scenario is, the sum utility optimized by the proposed algorithm is the best, when the PUs prefer the transmission rates completely, namely $\theta_1 = 1$ and $\theta_2 = 0$. Inversely, when only income is considered, namely $\theta_1 = 0$ and $\theta_2 = 1$, the optimized solution of all the PUs is the lowest. In detail, when $\varphi_1 \geq 0.2$ and $\theta_1 = 1$, the optimized solution is relatively higher.

As seen in Fig. 4, the relationships of the utility and adjustable factors are the same for the "Preferential Scenario" and "No-Preferential Scenario", when applying the proposed algorithm. Fig. 5 shows the gap of the utility optimized by the proposed algorithm for both scenarios. The value of θ_1 is the main factor influencing the gap of the optimized solution. Specifically, the performance of the "Preferential Scenario" and "No-Preferential Scenario" are identical at $\theta_1 = 0.3$. The performance of the "No-Preferential Scenario" is higher than that of the "Preferential Scenario" when $\theta_1 \leq 0.3$, and the gap is narrowing as θ_1 increases. By contrast, the performance

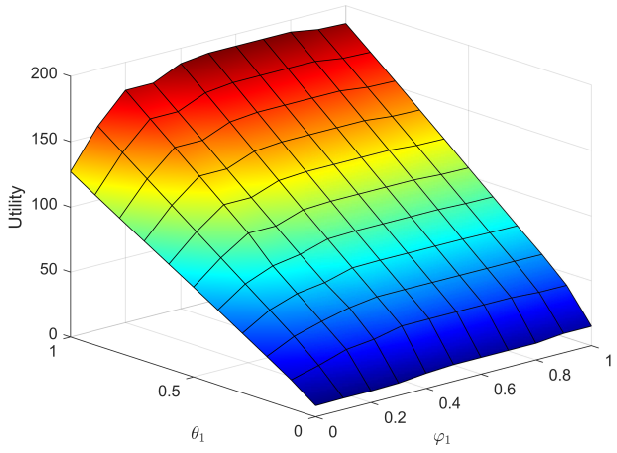

(a) Preferential Scenario

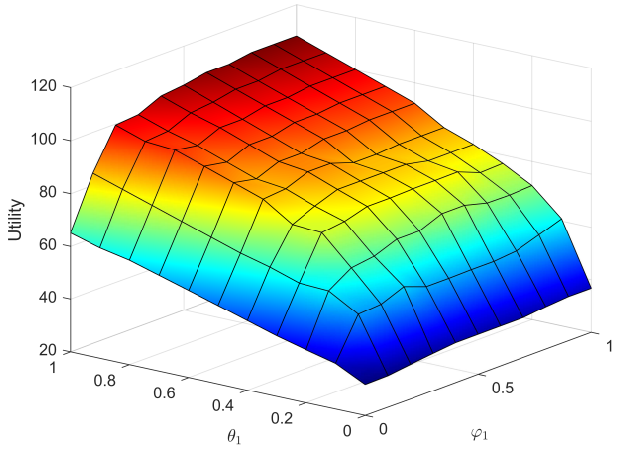

(b) No-Preferential Scenario

Fig. 4. The variation of the optimized solution with different adjustable factors, where $M = N = K = 25$, $T = 25$s, $\beta = 0.4$, $P_t = 25$ dBm.

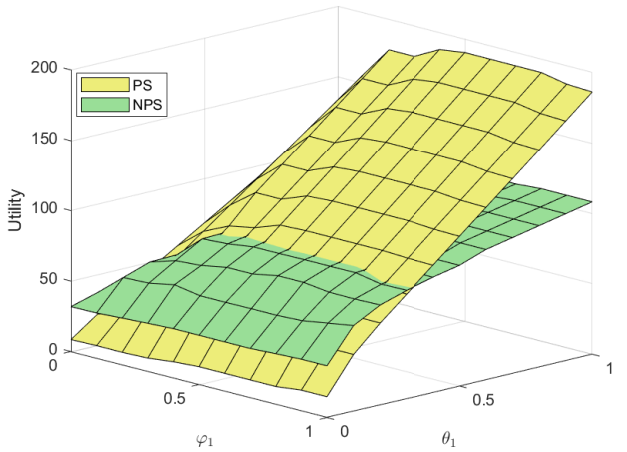

Fig. 5. The comparison of the optimized solution of the "Preferential Scenario" (PS) and "No-Preferential Scenario" (NPS), where $M = N = K = 25$, $T = 25$s, $\beta = 0.4$, $P_t = 25$ dBm.

of the "No-Preferential Scenario" is lower than that of the "Preferential Scenario" for $\theta_1 > 0.3$, and the gap is widening as θ_1 increases. In order to achieve the best utility of PUs, the 'Preferential Scenario' could be selected for solving the resource allocation problem when $\theta_1 > 0.3$, and the "No-Preferential Scenario" could be selected when $\theta_1 \leq 0.3$.

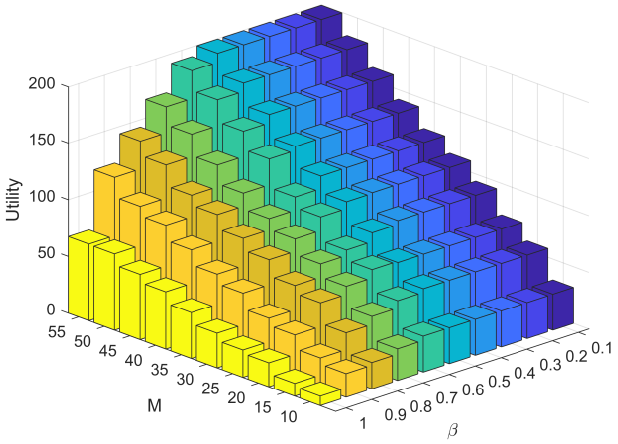

(a) Utility

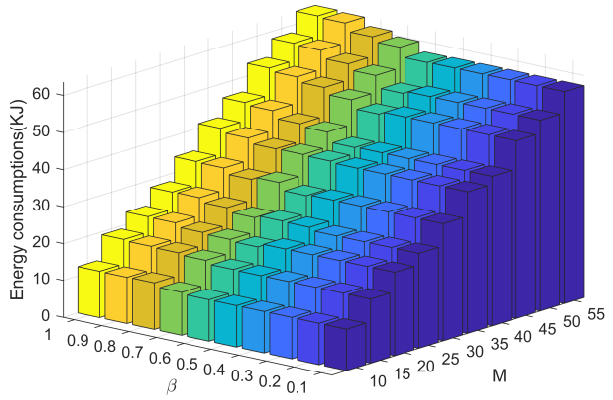

(b) Energy consumptions

Fig. 6. The variation of the optimized solution and energy consumptions with different rate regulation factors and numbers of PUs, where $M = N = K$, $T = M$ s, $\theta_1 = \theta_2 = 0.5$, $\varphi_1 = \varphi_2 = 0.5$, $P_t = 25$ dBm.

In the "No-Preferential Scenario", the utility factor φ_n^* of IoT Device n is related not only to the adjustable φ_1 and φ_2, but also to the rate regulation factor β. In Fig. 6, for different M, the relationships of the optimized solution, energy consumptions and the rate regulation factor β are investigated. Fig. 6(a) shows the variation of the optimized solution versus different M and β. No matter how many PUs there are, the optimized solution is near constant when $0.1 \leq \beta \leq 0.4$, and it decreases with the increasing of β when $0.5 \leq \beta \leq 1$. Furthermore, the energy consumptions are the lowest when $0.1 \leq \beta \leq 0.4$, and it increases with the increasing of β when $0.5 \leq \beta \leq 1$, as seen in Fig. 6(b). It can be concluded that the optimized solution and energy performances are the best, when the rate regulation factor β of each PU is $\beta \in [0.1, 0.4]$.

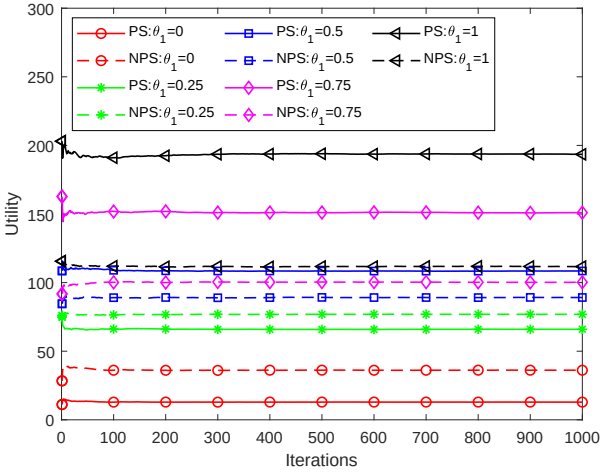

Fig. 7. The comparison of the convergence of the proposed algorithm under different adjustable factors θ_1 and θ_2, where $M = N = K = 25$, $T = 25$s, $\varphi_1 = \varphi_2 = 0.5$, $\beta = 0.4$, $P_t = 25$ dBm.

Fig. 7 investigates the convergence of the utility based resources sharing algorithm, and compares the performances of the proposed algorithm under different adjustable factors θ_1 and θ_2. No matter how much the adjustable factors are, the optimized solution converges to a stable value, when the iterations are more than 100. For $\theta_1 = 0$ and $\theta_2 = 0.25$, the convergence values of "No-Preferential Scenario", namely the optimized solution, are better than that of the "Preferential Scenario", and the difference between them decreases with the increasing of θ_1. For $\theta_1 = 0.5$, $\theta_1 = 0.75$ and $\theta_2 = 0.1$, the convergence values of "Preferential Scenario" are better than that of the "No-Preferential Scenario", and the difference between them increases with the increasing of θ_1. Furthermore, for both the two scenarios, the convergence values are the best, when $\theta_1 = 1$. The above analysis echoes that of Fig. 5.

The difference between the "Preferential Scenario" and "No-Preferential Scenario" is mainly in the transmission rates and income of PUs. Fig. 8 compares the rates and income of the "Preferential Scenario" to that of the "No-Preferential Scenario" considering $\theta_1 = 0$ and $\theta_2 = 1$. As shown in Fig. 8(a), the rates of the "Preferential Scenario" are better than that of the "No-Preferential Scenario", when the adjustable factors θ_1 and θ_2 are the same for both the two scenarios. Due to the fact that the transmission rates of PUs are improved by the matched IoT devices in the "Preferential Scenario", but that od the PUs are interfered by the matched IoT devices in the "No-Preferential Scenario", the rate performances of the "Preferential Scenario" are better. The transmission rates of PUs are the best in the "Preferential Scenario", where the PUs only consider the rates, namely $\theta_1 = 1$. Fig. 8(b) shows the income of PUs under different scenarios with different adjustable factors θ_1 and θ_2. In terms of the scenarios, the income of PUs of the "No-Preferential Scenario" is better than that of the "Preferential Scenario", regardless of the adjustable factors θ_1 and θ_2. In the "No-Preferential Scenario", there are

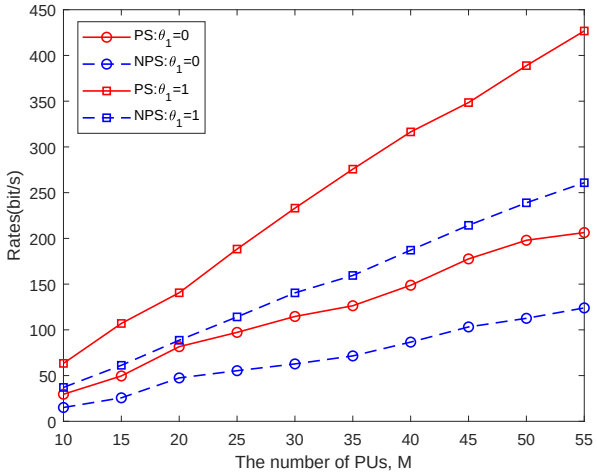

(a) Rate

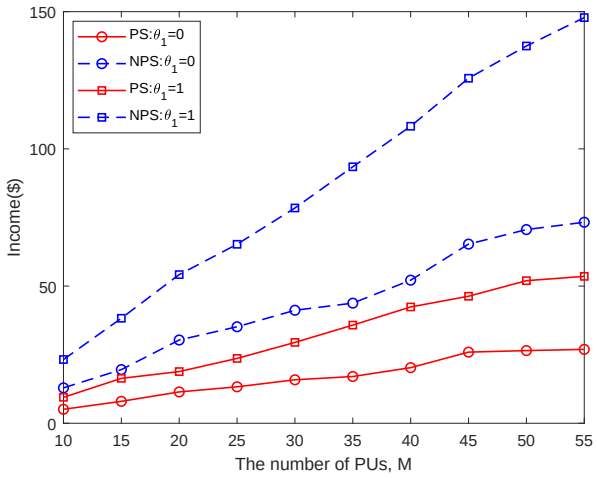

(b) Income

Fig. 8. The comparison of the rates and income of the PUs for the "Preferential Scenario" and "No-Preferential Scenario" under different adjustable factors θ_1 and θ_2, where $M = N = K$, $T = M$ s, $\varphi_1 = \varphi_2 = 0.5$, $\beta = 0.4$, $P_t = 25$ dBm.

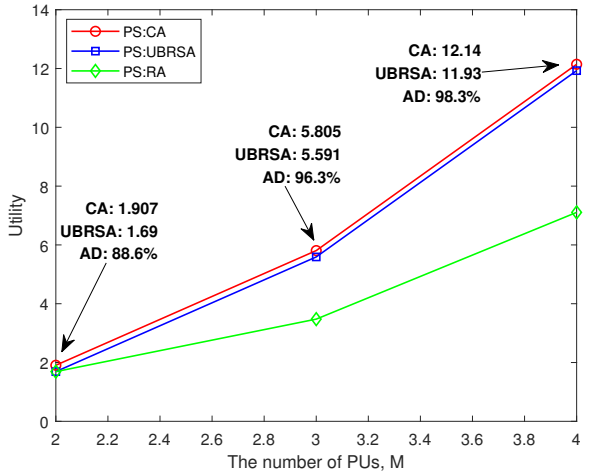

(a) Preferential Scenario

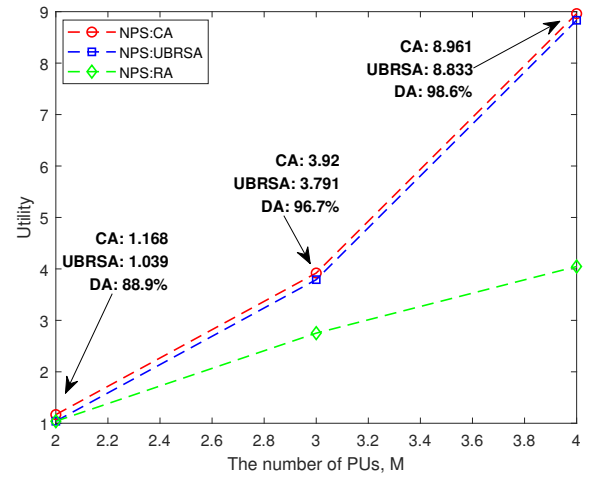

(b) No-Preferential Scenario

Fig. 9. The comparison of the utility optimized by different algorithms, where $M = N = K$, $T = M$ s, $\theta_1 = \theta_2 = 0.5$, $\varphi_1 = \varphi_2 = 0.5$, $\beta = 0.4$, $P_t = 25$ dBm.

no discounts for the IoT devices, so the income of PUs is higher than that of the "Preferential Scenario". The income of PUs is the best in the "No-Preferential Scenario", where the PUs only consider the rates, namely $\theta_1 = 1$. It can be concluded that each scenario has its own advantages, where the "Preferential Scenario" applying the proposed algorithm is good at optimizing the utility by improving the transmission rates of PUs, and the "No-Preferential Scenario" applying the proposed algorithm is good at optimizing the utility by improving the income of PUs.

Fig. 9 compares the optimized solution of the proposed algorithm to that of the centralized algorithm (CA) and random algorithm (RA) in the "Preferential Scenario" and "No-Preferential Scenario". The exhaustive search is required by the CA, and the complexity of CA is given by

$$O((M!)^2 M). \tag{64}$$

As shown in Fig. 9(a) and Fig. 9(b), the performance of the utility based resources sharing algorithm (UBRSA) is very close to that of the CA, and obviously better than that of the RA for both the "Preferential Scenario" and "No-Preferential Scenario". Specifically, as the number of users increases, the approximation degree (AD) between the optimized solutions of the proposed algorithm as well as the CA is always higher than 88%. It can be speculated that the approximation degree is close to 100% by considering the intensive users. In general, the proposed algorithm could obtain the approximate solutions of Eq. (29) and Eq. (52), where the approximation degree is always more than 88%.

The operation number of the proposed algorithm and CA are compared in Table. I. The operation number of CA in the "Preferential Scenario" and "No-Preferential Scenario" are identical for the same numbers of PUs M, and increase rapidly with the increasing of M. For the proposed UBRSA, the operation number in the "Preferential Scenario" is approximate with that in the "No-Preferential Scenario", and much lower

Operation number / Algorithm \ PUs number	M=5	M=10	M=15	M=20
UBRSA:PS	21	79	167	285
UBRSA:NPS	21	72	174	284
CA:PS&NPS	72000	1.3168e+14	2.5650e+25	1.1838e+38

TABLE I
THE COMPARISON OF THE OPERATION NUMBER OF UBRSA AND CA UNDER DIFFERENT SCENARIOS, WHERE $M = N = K$, $T = 25$S, $\varphi_1 = \varphi_2 = 0.5$, $\theta_1 = \theta_2 = 0.5$, $\beta = 0.4$, $P_t = 25$ DBM.

than that of the CA in both the two scenarios. The proposed algorithm can obtain the approximate solution with the low complexity in the "Preferential Scenario" and "No-Preferential Scenario".

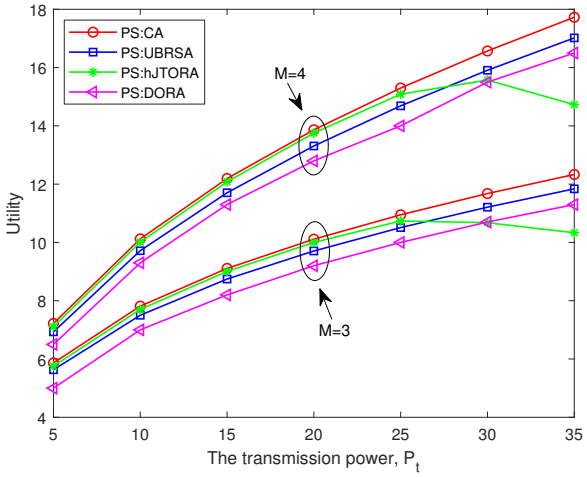

(a) Preferential Scenario

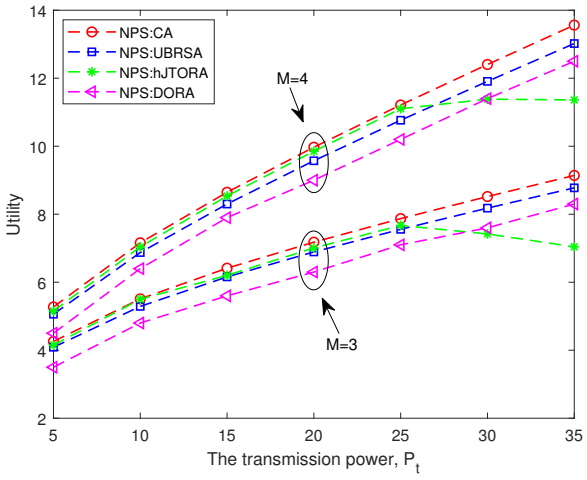

(b) No-Preferential Scenario

Fig. 10. The comparison of the optimized solution for the proposed algorithm and other algorithms, where $M = N = K$, $T = M$ s, $\theta_1 = \theta_2 = 0.5$, $\varphi_1 = \varphi_2 = 0.5$, $\beta = 0.4$.

To evaluate the performance of the proposed UBRSA further, the heuristic joint task offloading and resource allocation strategy (hJTORA) [49], as well as the distributed offloading and resource allocation (DORA) [50] are compared to the UBRSA as the increasing of the transmission power P_t, by implementing the "Preferential Scenario" and "No-Preferential Scenario". In the hJTORA, the task offloading and resource allocation problem is decomposed into a resource allocation (ReA) problem with fixed task offloading decision, a task offloading problem. Additionally, in the DORA, the convex and quasi-convex optimization techniques are used to allocate the communication resource, while offloading decision is solved by employing the sub-modular set function optimization method.

As shown in Fig. 10, the hJTORA attains the best utility performance of PUs by comparing with the UBRSA as well as the DORA, while the transmission power P_t is less than 25 dBm. When P_t is greater than 25 dBm, the performance of the hJTORA is decreasing. The performance of the proposed UBRSA is better than that of the DORA. Hence, the hJTORA is not applicable to the system requiring high energy, albeit the proposed UBRSA with the stable optimization ability can be able to implement for any system. Furthermore, the proposed algorithm is identical by considering different transmission power, and the approximation degree is always higher than 88%.

VII. CONCLUSION

In this paper, we have studied the resources sharing problem in a novel IoT, which applies the SR and EH techniques. In the conceived SR-aided IoT networks, both the PUs and IoT devices would like to offload tasks to the BS that is integrated with the MEC server. The IoT devices trade money with the PUs for communication resources. Considering the transaction modes between the PUs and IoT devices, we propose two cooperative scenarios (i.e., "Preferential Scenario" and "No-Preferential Scenario"). Furthermore, the utility maximization problems of the PUs for the proposed two scenarios are constructed, and we propose a utility based resources sharing algorithm to solve the problems in two scenarios. Our simulation and analysis results show that the proposed algorithm could obtain the stable approximate optimized solution of each cooperative scenario in the conceived networks. In addition, the "Preferential Scenario" has an advantage in improving the transmission rates of PUs, while the "No-Preferential Scenario" has the advantage in improving the income of PUs.

REFERENCES

[1] A. Zanella, N. Bui, A. Castellani, L. Vangelista, and M. Zorzi, "Internet of Things for Smart Cities," *IEEE Internet of Things Journal*, vol. 1, no. 1, pp. 22–32, 2014.
[2] A. Al-Fuqaha, M. Guizani, M. Mohammadi, M. Aledhari, and M. Ayyash, "Internet of Things: A Survey on Enabling Technologies, Protocols, and Applications," *IEEE Communications Surveys Tutorials*, vol. 17, no. 4, pp. 2347–2376, 2015.
[3] K. Shafique, B. A. Khawaja, F. Sabir, S. Qazi, and M. Mustaqim, "Internet of Things (IoT) for Next-Generation Smart Systems: A Review of Current Challenges, Future Trends and Prospects for Emerging 5G-IoT Scenarios," *IEEE Access*, vol. 8, pp. 23022–23040, 2020.
[4] Z. Lv, B. Hu, and H. Lv, "Infrastructure Monitoring and Operation for Smart Cities Based on IoT System," *IEEE Transactions on Industrial Informatics*, vol. 16, no. 3, pp. 1957–1962, 2020.
[5] C. Cabrera and S. Clarke, "A Self-Adaptive Service Discovery Model for Smart Cities," *IEEE Transactions on Services Computing*, vol. 15, no. 1, pp. 386–399, 2022.

[6] Q. Wu, W. Chen, D. W. K. Ng, and R. Schober, "Spectral and Energy-Efficient Wireless Powered IoT Networks: NOMA or TDMA?," *IEEE Transactions on Vehicular Technology*, vol. 67, no. 7, pp. 6663–6667, 2018.

[7] A. Nauman, Y. A. Qadri, M. Amjad, Y. B. Zikria, M. K. Afzal, and S. W. Kim, "Multimedia Internet of Things: A Comprehensive Survey," *IEEE Access*, vol. 8, pp. 8202–8250, 2020.

[8] W. Lu, S. Hu, X. Liu, C. He, and Y. Gong, "Incentive Mechanism Based Cooperative Spectrum Sharing for OFDM Cognitive IoT Network," *IEEE Transactions on Network Science and Engineering*, vol. 7, no. 2, pp. 662–672, 2020.

[9] W. Lu, P. Si, G. Huang, H. Han, L. Qian, N. Zhao, and Y. Gong, "SWIPT Cooperative Spectrum Sharing for 6G-Enabled Cognitive IoT Network," *IEEE Internet of Things Journal*, vol. 8, no. 20, pp. 15070–15080, 2021.

[10] N. Van Huynh, D. T. Hoang, X. Lu, D. Niyato, P. Wang, and D. I. Kim, "Ambient Backscatter Communications: A Contemporary Survey," *IEEE Communications Surveys Tutorials*, vol. 20, no. 4, pp. 2889–2922, 2018.

[11] M. Z. Chowdhury, M. Shahjalal, S. Ahmed, and Y. M. Jang, "6G Wireless Communication Systems: Applications, Requirements, Technologies, Challenges, and Research Directions," *IEEE Open Journal of the Communications Society*, vol. 1, pp. 957–975, 2020.

[12] P. X. Nguyen, D.-H. Tran, O. Onireti, P. T. Tin, S. Q. Nguyen, S. Chatzinotas, and H. Vincent Poor, "Backscatter-Assisted Data Offloading in OFDMA-Based Wireless-Powered Mobile Edge Computing for IoT Networks," *IEEE Internet of Things Journal*, vol. 8, no. 11, pp. 9233–9243, 2021.

[13] Z. Liu, S. Zhao, Y. Yang, K. Ma, and X. Guan, "Towards Hybrid Backscatter-aided Wireless Powered Internet of Things Networks: Cooperation and Coexistence Scenarios," *IEEE Internet of Things Journal*, pp. 1–1, 2021.

[14] X. Li, M. Zhao, M. Zeng, S. Mumtaz, V. G. Menon, Z. Ding, and O. A. Dobre, "Hardware Impaired Ambient Backscatter NOMA Systems: Reliability and Security," *IEEE Transactions on Communications*, vol. 69, no. 4, pp. 2723–2736, 2021.

[15] U. S. Toro, K. Wu, and V. C. M. Leung, "Backscatter Wireless Communications and Sensing in Green Internet of Things," *IEEE Transactions on Green Communications and Networking*, vol. 6, no. 1, pp. 37–55, 2022.

[16] X. Lu, P. Wang, D. Niyato, D. I. Kim, and Z. Han, "Wireless Networks With RF Energy Harvesting: A Contemporary Survey," *IEEE Communications Surveys Tutorials*, vol. 17, no. 2, pp. 757–789, 2015.

[17] D. Niyato, D. I. Kim, M. Maso, and Z. Han, "Wireless Powered Communication Networks: Research Directions and Technological Approaches," *IEEE Wireless Communications*, vol. 24, no. 6, pp. 88–97, 2017.

[18] M. A. Ullah, R. Keshavarz, M. Abolhasan, J. Lipman, K. P. Esselle, and N. Shariati, "A Review on Antenna Technologies for Ambient RF Energy Harvesting and Wireless Power Transfer: Designs, Challenges and Applications," *IEEE Access*, vol. 10, pp. 17231–17267, 2022.

[19] Z. Chu, P. Xiao, D. Mi, W. Hao, Z. Lin, Q. Chen, and R. Tafazolli, "Wireless Powered Intelligent Radio Environment with Non-Linear Energy Harvesting," *IEEE Internet of Things Journal*, pp. 1–1, 2022.

[20] Y. Zhang, X. Liu, K. Zheng, Y. Li, and Y. Yao, "Energy-efficient Multi-codebook Based Backscatter Communications for Wireless Powered Networks," *IEEE Internet of Things Journal*, pp. 1–1, 2022.

[21] H. Xiao, H. Jiang, L.-P. Deng, Y. Luo, and Q.-Y. Zhang, "Outage Energy Efficiency Maximization for UAV-Assisted Energy Harvesting Cognitive Radio Networks," *IEEE Sensors Journal*, vol. 22, no. 7, pp. 7094–7105, 2022.

[22] S. Haykin, "Cognitive radio: brain-empowered wireless communications," *IEEE Journal on Selected Areas in Communications*, vol. 23, no. 2, pp. 201–220, 2005.

[23] I. F. Akyildiz, W.-y. Lee, M. C. Vuran, and S. Mohanty, "A survey on spectrum management in cognitive radio networks," *IEEE Communications Magazine*, vol. 46, no. 4, pp. 40–48, 2008.

[24] W. S. H. M. W. Ahmad, N. A. M. Radzi, F. S. Samidi, A. Ismail, F. Abdullah, M. Z. Jamaludin, and M. N. Zakaria, "5G Technology: Towards Dynamic Spectrum Sharing Using Cognitive Radio Networks," *IEEE Access*, vol. 8, pp. 14460–14488, 2020.

[25] D. K. Jasim and S. B. Sadkhan, "Cognitive Radio Network: Security and Reliability trade-off - Status, Challenges, and Future trend," in *2021 1st Babylon International Conference on Information Technology and Science (BICITS)*, pp. 149–153, 2021.

[26] Y. Pei, Y.-C. Liang, K. C. Teh, and K. H. Li, "Energy-Efficient Design of Sequential Channel Sensing in Cognitive Radio Networks: Optimal Sensing Strategy, Power Allocation, and Sensing Order," *IEEE Journal on Selected Areas in Communications*, vol. 29, no. 8, pp. 1648–1659, 2011.

[27] F. Wang, M. Krunz, and S. Cui, "Price-Based Spectrum Management in Cognitive Radio Networks," *IEEE Journal of Selected Topics in Signal Processing*, vol. 2, no. 1, pp. 74–87, 2008.

[28] D. Xu, X. Yu, Y. Sun, D. W. K. Ng, and R. Schober, "Resource Allocation for IRS-Assisted Full-Duplex Cognitive Radio Systems," *IEEE Transactions on Communications*, vol. 68, no. 12, pp. 7376–7394, 2020.

[29] T. Nadkar, V. Thumar, G. Shenoy, A. Mehta, U. B. Desai, and S. N. Merchant, "A cross-layer framework for symbiotic relaying in cognitive radio networks," in *2011 IEEE International Symposium on Dynamic Spectrum Access Networks (DySPAN)*, pp. 498–509, 2011.

[30] T. Huang, W. Yang, J. Wu, J. Ma, X. Zhang, and D. Zhang, "A Survey on Green 6G Network: Architecture and Technologies," *IEEE Access*, vol. 7, pp. 175758–175768, 2019.

[31] Q. Zhang, L. Zhang, Y.-C. Liang, and P.-Y. Kam, "Backscatter-NOMA: A Symbiotic System of Cellular and Internet-of-Things Networks," *IEEE Access*, vol. 7, pp. 20000–20013, 2019.

[32] Y.-C. Liang, Q. Zhang, E. G. Larsson, and G. Y. Li, "Symbiotic Radio: Cognitive Backscattering Communications for Future Wireless Networks," *IEEE Transactions on Cognitive Communications and Networking*, vol. 6, no. 4, pp. 1242–1255, 2020.

[33] Z. Xu, G. Hu, M. Jia, and L. Dong, "Potential transmission choice for Internet of Things (IoT): Wireless and batteryless communications and open problems," *China Communications*, vol. 18, no. 2, pp. 241–249, 2021.

[34] R. Long, Y.-C. Liang, H. Guo, G. Yang, and R. Zhang, "Symbiotic Radio: A New Communication Paradigm for Passive Internet of Things," *IEEE Internet of Things Journal*, vol. 7, no. 2, pp. 1350–1363, 2020.

[35] Y. Liu, P. Ren, and Q. Du, "Symbiotic Communication: Concurrent Transmission for Multi-Users Based on Backscatter Communication," in *2020 International Conference on Wireless Communications and Signal Processing (WCSP)*, pp. 835–839, 2020.

[36] Q. Zhang, Y.-C. Liang, and H. V. Poor, "Intelligent User Association for Symbiotic Radio Networks Using Deep Reinforcement Learning," *IEEE Transactions on Wireless Communications*, vol. 19, no. 7, pp. 4535–4548, 2020.

[37] Q. Zhang, Y.-C. Liang, and H. V. Poor, "Reconfigurable Intelligent Surface Assisted MIMO Symbiotic Radio Networks," *IEEE Transactions on Communications*, vol. 69, no. 7, pp. 4832–4846, 2021.

[38] L. Qian, Y. Wu, J. Ouyang, Z. Shi, B. Lin, and W. Jia, "Latency Optimization for Cellular Assisted Mobile Edge Computing via Non-Orthogonal Multiple Access," *IEEE Transactions on Vehicular Technology*, vol. 69, no. 5, pp. 5494–5507, 2020.

[39] S. Wang, M. Chen, X. Liu, C. Yin, S. Cui, and H. Vincent Poor, "A Machine Learning Approach for Task and Resource Allocation in Mobile-Edge Computing-Based Networks," *IEEE Internet of Things Journal*, vol. 8, no. 3, pp. 1358–1372, 2021.

[40] H. Yang, Z. Wei, Z. Feng, X. Chen, Y. Li, and P. Zhang, "Intelligent Computation Offloading for MEC-Based Cooperative Vehicle Infrastructure System: A Deep Reinforcement Learning Approach," *IEEE Transactions on Vehicular Technology*, vol. 71, no. 7, pp. 7665–7679, 2022.

[41] T. Kim, D. J. Love, and B. Clerckx, "Does Frequent Low Resolution Feedback Outperform Infrequent High Resolution Feedback for Multiple Antenna Beamforming Systems?," *IEEE Transactions on Signal Processing*, vol. 59, no. 4, pp. 1654–1669, 2011.

[42] L. Liang, J. Kim, S. C. Jha, K. Sivanesan, and G. Y. Li, "Spectrum and Power Allocation for Vehicular Communications With Delayed CSI Feedback," *IEEE Wireless Communications Letters*, vol. 6, no. 4, pp. 458–461, 2017.

[43] K. Wang, F. Fang, D. B. d. Costa, and Z. Ding, "Sub-Channel Scheduling, Task Assignment, and Power Allocation for OMA-Based and NOMA-Based MEC Systems," *IEEE Transactions on Communications*, vol. 69, no. 4, pp. 2692–2708, 2021.

[44] Z. Ding, L. Lv, F. Fang, O. A. Dobre, G. K. Karagiannidis, N. Al-Dhahir, R. Schober, and H. V. Poor, "A State-of-the-Art Survey on Reconfigurable Intelligent Surface-Assisted Non-Orthogonal Multiple Access Networks," *Proceedings of the IEEE*, pp. 1–22, 2022.

[45] L. Lv, Q. Wu, Z. Li, Z. Ding, N. Al-Dhahir, and J. Chen, "covert communication in intelligent reflecting surface-assisted noma systems: Design, analysis, and optimization," *IEEE Transactions on Wireless Communications*.

[46] D. Ng, "Three-dimentionl stable matching problems," 2014.

[47] S. Wen, W. Liang, J. Cui, D. Wang, and L. Li, "Resource Allocation Based on Three-Sided Matching Theory in Cognitive Vehicular Networks," in *2021 IEEE 94th Vehicular Technology Conference (VTC2021-Fall)*, pp. 1–6, 2021.

[48] N. Raveendran, Y. Gu, C. Jiang, N. H. Tran, M. Pan, L. Song, and Z. Han, "Cyclic Three-Sided Matching Game Inspired Wireless Network Virtualization," *IEEE Transactions on Mobile Computing*, vol. 20, no. 2, pp. 416–428, 2021.

[49] T. X. Tran and D. Pompili, "Joint Task Offloading and Resource Allocation for Multi-Server Mobile-Edge Computing Networks," *IEEE Transactions on Vehicular Technology*, vol. 68, no. 1, pp. 856–868, 2019.

[50] X. Lyu, H. Tian, C. Sengul, and P. Zhang, "Multiuser Joint Task Offloading and Resource Optimization in Proximate Clouds," *IEEE Transactions on Vehicular Technology*, vol. 66, no. 4, pp. 3435–3447, 2017.